Feasibility of Microbial-Induced Calcite Precipitation in soils polluted by hydrocarbons

Authors: Carla Comadran-Casas[1]*, Philip J. Salter [2], Ayo Ogundero[1], Fabien Cholet[1], Victor Barridor Giadom[1], William Sloan[1], Adrian M. Bass[3], John Macdonald[3], Cise Unluer[4], Caroline Gauchotte-Lindsay[1]

[1] James Watt School of Engineering, the University of Glasgow, United Kingdom

[2] Department of Civil & Environmental Engineering University of Strathclyde, Glasgow, United Kingdom

[3] School of Geographical & Earth Sciences, University of Glasgow, Glasgow, United Kingdom

[4] Department of Civil Engineering and Management, University of Manchester, Manchester, United Kingdom

Corresponding author: Carla.ComadranCasas@glasgow.ac.uk

Abstract

This study presents an investigation on the potential of biostimulation and bioaugmentation of Microbial-Induced Calcite Precipitation (MICP) in soils polluted by polycyclic aromatic hydrocarbons (PAH). Biostimulation of urea hydrolysis by soil autochthonous ureolytic bacteria was not detected over 62 days. Flow cytometry revealed *Sproposarcina pasteurii* at initial OD_{600} = 0.01 was able to grow in soil water extracts of increasing hydrocarbon concentration (TOC = 0.035-35 mg/L), showing no negative effects on cell membrane stability. Urease activity assays in soil water extracts inoculated with *S. pasteurii* (OD_{600} = 0.01 and 1) and soybean *Glycine Max* urease enzyme (1 and 100 g/L) indicated cell and enzyme urease inhibition was dependant on hydrocarbon and cell/enzyme concentrations. *Glycine Max* urease activity was unaffected at 100 g/L but at 1 g/L decreased with increasing hydrocarbon concentration up to 61%. *S. pasteurii* at OD_{600} = 1 readily decreased at the lowest hydrocarbon concentration (TOC = 0.35 mg/L) to an overall reduction of 31% at the highest concentration. Bioaugmentation of *S. pasteurii* ($OD_{600, initial}$ = 1) inoculated in the soil matrix successfully hydrolysed urea within 24 h. These results evidence for the first time the ability of model MICP bacteria *S. pasteurii* to grow and maintain relevant metabolic ureolytic activity in soils significantly polluted by PAH.

Keywords: urea hydrolysis, urease activity, microbial-induced calcite precipitation, polycyclic aromatic hydrocarbons, organic contaminants, soil, biostimulation, bioaugmentation

Synopsis: Microbial-Induced Calcite Precipitation (MICP) in soils polluted by organic contaminants is poorly understood. This research evidence the feasibility of MICP in soils heavily polluted by polycyclic aromatic hydrocarbons.

1. Introduction

Soil contaminants including trace elements (e.g., Cd, Pb, Cu, Zn, As), radionuclides (e.g., ^{90}Sr), organic pollutants (e.g., hexachlorocyclohexanes, polycyclic aromatic hydrocarbons, polychlorinated biphenyls, polybrominated diphenyl ethers) and emerging contaminants (e.g., pharmaceuticals, plastics, nanomaterials) are a global pressing issue with severe negative effects both on the environment and humans[1]. An effective bioremediation method for heavy metals is their immobilisation via incorporation into calcium carbonate ($CaCO_3$) minerals through Microbial-Induced Calcite Precipitation (MICP) where toxic elements (e.g. Cr^{6+}[2, 3, 4], Pb^{2+}[5, 6], Sr^{2+}[7], Cd^{2+}[8, 9], Zn^{2+}[8, 9], As^{3+}[10], Ni^{2+}[11], Cu^{2+}[12]) can substitute for calcium (Ca^{2+}), forming stable and insoluble phases. An important unexplored avenue of MICP in the context of bioremediation is its feasibility in soils polluted by organic contaminants. High molecular weight persistent organic pollutants such as polycyclic aromatic hydrocarbons (PAHs) accumulate on surficial soils near source points[13], resulting in higher concentrations in industrial and urban centres[14] where they co-exist with heavy metals[15].

MICP requires abundance of carbonate (CO_3^{2-}) and calcium (Ca^{2+}) ions and an alkaline pH (>8.5). These conditions are achieved through multiple bacterial metabolic pathways (ammonification, denitrification, sulphate and iron reduction)[16]. Ammonification of urea, or urea hydrolysis, is mostly studied due to ubiquitousness of bacteria[17] and robustness against environmental conditions[18,19, 20, 21]. Ureolytic bacteria catalyse the hydrolysis of urea into ammonia and carbamic acid through the urease enzyme (1). Carbamic acid spontaneously hydrolyses into ammonia and carbonic acid (H_2CO_3) **Error! Reference source not found.**, which subsequently equilibrate with water as bicarbonate (HCO_3^-) and ammonium (NH_4^+) ions (Eqs. (3) and (4). The excess of hydroxide ions (OH^-) between pH 6.3 and 9.3 (pK_1 and pK_a, respectively) results in a net increase in pH, shifting HCO_3^- speciation to CO_3^{2-}. Given the presence of Ca^{2+}, $CaCO_3$ precipitation ensues (5)[22].

$$CO(NH_2)_2 + 2H_2O \xrightarrow{urease} NH_3 + NH_2COOH \quad (1)$$

$$NH_2COOH + H_2O \rightarrow NH_3 + H_2CO_3 \quad (2)$$

$$H_2CO_3 \leftrightarrow H^+ + HCO_3^- \quad (3)$$

$$2NH_3 + 2H^+ \leftrightarrow 2NH_4^+ + 2OH^- \quad (4)$$

$$Ca^{2+} + HCO_3^- + OH^- \leftrightarrow CaCO_3 + H_2O \quad (5)$$

In soils polluted by organic contaminants, urease activity has been investigated as a biomarker to assess soil pollution. Petroleum hydrocarbons have been shown to stimulate[23, 24, 25, 26, 27] and impair[28, 29; 27; 30, 31] soil urea hydrolysis. This has been shown to be dependent on pollutant concentration[28, 31], type of hydrocarbon[26, 32], co-presence of inorganic pollutants (e.g., heavy metals)[30, 33] as well as soil properties (e.g., total organic carbon, pH)[27], nutrient availability (e.g., phosphorous)[24], and incubation time[26, 30].

Little is known about the effects of PAH on ureolytic bacteria at molecular scale. Inhibition of urea hydrolysis may occur at cell and/or enzyme level, yet the exact mechanisms remain unclear. At cell level, it has been postulated that lipophilic compounds such as PAH have a narcotic mode of toxic action on bacteria, interacting with lipophilic components of bacteria cytoplasmatic membranes and affecting their permeability and structure[34, 35]. Narcosis is produced by non-specific binding of pollutants to cell membranes, dissolving or disrupting their fluidity and function and hence is dependent on pollutant lipophilicity[36]. At enzyme level, organic compounds are thought to denature the entire protein structure[30] and additionally cause loss of catalytic function through interaction with functional groups of the enzyme active site and residues critical to maintaining its conformation[37].

Understanding the effect of persistent organic pollutants on MICP is important in developing applications in bioremediation and biogeotechnics due to their widespread presence and co-existence with other pollutants (e.g., heavy metals) in environments of anthropogenic and ecological relevance. Towards this goal, this study aimed to elucidate MICP's feasibility in presence of PAH by investigating their effect on ureolytic bacteria growth and ureolysis. Firstly, we investigated the response of a soil from a gas plant heavily polluted by PAH to the application of urea over two months to determine the feasibility of MICP biostimulation approaches. Secondly, we investigated the viability of model MICP bacteria *S. pasteurii* growth in PAH polluted soil extracts at varying PAH concentrations to determine its potential to thrive once introduced in the polluted environment. Thirdly, we conducted urease activity assays in PAH polluted soil water extracts at varying cell, urease enzyme and PAH concentrations, under the hypothesis of increasing urease activity inhibition with increasing hydrocarbon concentration. The inhibitory effect of PAH on urease activity was investigated on *S. pasteurii* and soybean (*Glycine Max)* extracted plant urease to elucidate inhibition mechanisms at cell and enzyme level. Ureases exhibit high homology of amino acid sequencies across species, such that the active site is conserved and induces the same mechanism of catalytic activity[38], making plant and bacterial urease activity assays adequate to investigate inhibition mechanisms at cell and enzyme level. Based on the obtained results, we induced bioaugmentation of *S. pasteurii* on the PAH polluted soil. The

results of this study provide, for the first time, scientific evidence of the feasibility of MICP in soil environments polluted by PAH.

2. Materials and methods

2.1 Soils

A soil polluted by coal tar (COV14) was sourced from a gas plant (England, UK) in which the main contaminants are PAH as described in Gauchotte-Lindsay et al. [40]. An uncontaminated reddish sand from a quarry near Glasgow (GQ, Garnock Quarry, Hugh King & Co Scotland, UK) was used as a control, whose mineralogical, chemical and physical properties are described in Comadran-Casas et al. [41].

2.2. Soil hydrocarbon water extraction

Earlier studies have evidenced that only the fraction of substance (i.e., PAH) dissolved in pore water is available to bacteria[36], therefore soil water extractions were deemed suitable to reduce the complexity of soil matrices. The soil was sieved <2 mm in sterile conditions and stored in the fridge (4°C) until further use. A soil extract containing extractable organic contaminants was obtained by placing COV14 soil and autoclaved ultrapure water (Milli-Q water filtration system Elga Purelab Chorus, from here onwards “DI”) in a 100 mL borosilicate reagent glass bottle at a soil to liquid ratio of 1:2.5, topping it up to make sure no air remained in the bottle, mixed thoroughly, and placed in an orbital shaker at 200 rpm for 18 h. Subsequently the sample was stored in the dark for 3 days for equilibration[42]. The soil extract was obtained by vacuum assisted filtration through 0.2 µm glass filter, obtaining a stock solution which was subsequently transferred to a reagent borosilicate glass bottle and stored in the fridge at 4°C until further use. Glass bottles were previously rinsed thoroughly with deionised water, baked at 550°C and autoclaved. A sample of the 1:2.5 COV14 extract was analysed for total dissolved carbon as specified in 2.9.4. The soil extract was diluted 1:5, 1:10, 1:100 and 1:1000 with DI water to provide a range of hydrocarbon content.

2.3. *Glycine Max* urease extraction

Glycine Max (soybean, Whole food earth, Kent, UK) beans were soaked overnight (>12 h) in DI water at a bean to water mass to volume proportion of 100 g/L. The mixture was blended for 5 min and stirred for 30 min in an orbital shaker at 200 rpm. In sterile conditions, $CaSO_4 \cdot 2H_2O$ (>99.5% ACS reagent, Fisher Scientific) was added to the mixture at a 1:10 beans weight ratio, stirred for another 5 min, and allowed to rest for 1 h to induce solid coagulation. The mixture was then decanted into 50 mL centrifuge tubes in sterile conditions

and centrifuged at 3000 rpm overnight at 4°C. The supernatant was subsequently filtered through 0.2 µm cellulose filter (Sartorius Minisart) into borosilicate glass bottles, obtaining a 100 g/L stock urease solution, which was stored in the freezer (-20°C) until further use. The 100 g/L urease stock solution was diluted to 1 g/L with DI water and stored in the freezer at -20°C until use. Glass bottles were previously rinsed thoroughly with DI water, baked at 550°C and autoclaved.

2.4. *Sporosarcina pasteurii* culture

S. pasteurii DSM 33 was grown for 24 h in an orbital shaker incubator set at 30ºC and 150 rpm in LBU media containing 10 g/L tryptone (Formedium Ltd.), 10 g/L NaCl (≥99.0%, ACS reagent, Sigma Aldrich), 5 g/L yeast extract powder (Formedium Ltd.) and 20 g/L urea (≥99.5% ACS reagent, Fisher Scientific) adjusted to pH 7 with NaOH and filter sterilised through 0.2 µm. Bacteria were pelleted by centrifugation at 30 min and 2500 g, resuspended in autoclaved 5 g/L NaCl solution and diluted to OD_{600} of 0.01 or 1. The optical density was measured at 600 nm with a spectrophotometer (DR 1900, Hach). This procedure was conducted daily prior to experimentation.

2.5. Soil DNA extraction and detection of relevant genes for bioremediation

COV14 soil DNA was extracted with the RNeasy PowerSoil Total RNA Kit plus DNA Elution Kit (Qiagen) according to the manufacturer's instructions. PCR annealing temperature was optimised for target genes of bacterial ureolysis (ureC) using soil environmental DNA and tested on soil COV14 environmental DNA as template. Genes were amplified using primers listed in Table 1 with a HotStarTaq Polymerase kit (Qiagen) in a 50 µL final volume composed of 5 µL 10x PCR buffer (15 mM $MgCl_2$), 39.75 µL PCR water, 1 µL of each primer (10 µM, Eurofins), 1 µL dNTPs (10 µM each), 0.25 µL HotStarTaq DNA polymerase and 2 µL of DNA sample. PCR conditions were as follow: 95ºC for 15 min, (94ºC 30 s, T_m*ºC 30 s, 72ºC 30 s) × 30 and 72ºC 10 min, where T_m* is the optimum annealing temperatures determined through gradient PCR (**Table 1**) combined with agarose gel electrophoresis to separate PCR products.

Table 1 List of ureC primers used in this study to test the presence of ureC gene in extracted environmental soil DNA and optimum annealing temperatures (T_m*).

Primer	Sequence (5' → 3')	Orientation	Target	Length (bp)	Reference	T_m* (°C)
ureC-F	AAGSTSCACGAGGACTGGGG	Forward	Bacterial ureC	318	[43]	57
ureC-R	AGGTGGTGGCASACCATSAGCAT	Reverse				

ureC-L2F	ATHGGYAARGCNGGNAAYCC	Forward	Bacterial ureC	408	[44]	-
ureC-L2R	GTBSHNCCCCARTCYTCRTG	Reverse				
ureC607F	AARMTSCAYGARGACTGGGG	Forward	Bacterial ureC	310	[45]	56
ureC898R	TGRCASACCATSAKCATGTC	Reverse				

2.6. Soil urea hydrolysis through biostimulation and bioaugmentation

The potential to induce urea hydrolysis through biostimulation of autochthonous ureolytic bacteria was investigated in COV14 soil samples and on an uncontaminated quarry sand (GQ) which served as control. Samples were prepared by adding 2 g of soil (<2 mm) in sterile RNAase free15 mL centrifuge tubes (Sarstedt AG&Co KG). Following preparation, 4 mL treatment solution were pipetted, and tubes were closed and thoroughly shaken to mix soil and solution, marking t = 0. Both sample preparation and treatment application were conducted in sterile conditions. The treatment solution was prepared adding 333 mM urea, 10 g/L ammonium chloride (NH_4Cl, >99.5% Acros Organics) and 3 g/L nutrient broth (Nutriselect basic, Sigma Aldrich) to DI water, filter sterilised through sterile 0.2 µm cellulose syringe filters, transferred into pre-autoclaved borosilicate glass bottles in sterile conditions and stored at 4ºC until use. Samples were subsequently transferred into an incubator set at room temperature (20±3ºC) with gentle shaking (150 rpm) and allowed to react in closed vials and dark conditions for up to 2 months. Samples were taken at reaction times (t_r) = 0, 1, 2, 3, 4, 10, 20, 30 and 62 days. Bioaugmentation experiments were conducted on COV14 soil only. Soil samples were prepared as in biostimulation experiments. *S. pasteurii* was grown to an OD_{600} = 1 as indicated in Section 2.4 and resuspended in sterile PBS buffer. Soils were treated with 2 mL of LBU media containing x2 the mass proportion of chemical compounds and 2 mL of *S. pasteurii*. Samples were obtained at t_r = 0, 1, 2, 3 and 7 days. Three replicate samples were prepared for each reaction time point. Following reaction time, samples were centrifuged at 2500 g for 20 min to separate soil and solution. The solution was subsequently decanted and filtered through 0.2 µm for analysis of pH and NH_4^+ (see Section 2.9.1 and 2.9.2).

2.7. Viability assay

To determine whether *S. pasteurii* could grow and maintained cell membrane structure in the presence of organic contaminants a viability experiment was conducted. *S. pasteurii* was grown overnight and diluted to an initial OD_{600} = 0.01 as in Section 2.4. Growth solutions were prepared by adding x2 the mass proportion of chemical compounds of LBU media into

soil extract solutions. Growth media were prepared in borosilicate glass bottles previously rinsed with DI water and baked at 550ºC. Following media preparation growth solutions were filter sterilised. Equal volumes of *S. pasteurii* stock solution and growth solutions containing increasing concentration of organic contaminants were pipetted to RNAse free sterile 15 mL centrifuge tubes, mixed thoroughly, and placed in an orbital shaker incubator at 150 rpm and T = 30ºC. Samples were obtained at t = 0, 2, 4, 8, 12, 20 and 24 h. Sampling was destructive such that three replicates were prepared for each hydrocarbon concentration and reaction time point.

Methods to study bacteria growth and kinetics have typically involved optical density or cell dry weight[46] which are indirect measurements of cell concentration and can be misleading when trying to determine bacteria viability nor provide information on cell membrane stability[47, 48]. In this study we employed flow cytometry which provides direct measurement of total cell counts and has been used to differentiate total from intact cell counts through the use of stains that penetrate or not cell membranes, from which cell viability and membrane structure can be inferred[49, 50].

Quantification of bacteria population was performed using the Cytoflex flow cytometer (Beckman Coulter). Samples were prepared by cell fixation with glutaraldehyde (1% in DI water) and diluted as necessary with filtered (0.22 µm Sartorius™ Minisart™ Plus Syringe Filters, Fisher scientific) DI water[51]. Samples were stained for total and intact cell count with 10 µL/mL of SYBR Green I (SGI) and 10 µL/mL of SYBR Green I mixed with propidium iodide (SGI/PI), respectively, and incubated in the dark for 15 min before measurement. The total cell stain was prepared by diluting the stock solution of SGI (10,000 x in DMSO, Thermofisher) 1:100 in EDTA (1 mM) and the intact cell stain by mixing SGI with PI (1.6 mM) and diluting 1:100 in EDTA (1 mM) for a final concentration of 0.6 mM PI and 100x for SGI. Gating was used to distinguish the selected bacteria population background with the aid of negative controls consisting of the DI water used for dilutions, growth solutions composed of LBU in soil extracts and filtered samples (<0.22 µm) to remove any bacterial cells using the software CytExpert (Beckman Coulter).

The bacteria specific growth rate was estimated by fitting a regression line to the logarithmic cell counts during the exponential growth phase, with the slope of the line representing the growth rate. The lag phase duration was estimated as the x-axis intercept of the regression line, assuming a theoretical extrapolation from the exponential phase[52].

2.8. Urease activity assay

To investigate organic contaminant effect on urease activity at enzyme and cell level, extracted *Glycine Max* urease (1 and 100 g/L) and *S. pasteurii* (OD_{600} = 0.01 and 1) were exposed to increasing concentrations of COV14 soil extracts obtained as indicated in Section 2.2 to which 666 mM urea were added in a 1:1 volume ratio. The higher enzyme and cell concentrations were chosen for comparative purposes with previous studies providing similar enzyme and cell urease activity rates[53, 54]. Positive controls included *Glycine Max* urease and *S. pasteurii* exposed to solutions containing no contaminants but 666 mM urea or 666 mM urea plus 5 g/L NaCl, respectively. Negative controls were run on COV14 extracts containing 666 mM urea, 666 mM urea, and 666 mM urea plus 5 g/L NaCl solutions, where *Glycine Max* urease or *S. pasteurii* solutions were replaced by DI water.

The urease activity (UA) was determined through changes in electrical conductivity (EC) over time with measurements taken every 0.5 min over 20 min[55] by adding equal volumes of either *Glycine Max* urease or *S. pasteurii* and COV14 soil extracts plus urea in glass vials. Glass vials previously rinsed with DI water and baked at 550ºC overnight. The UA was computed as:

$$UA\left(\frac{\mu M}{min}\right) = \frac{\Delta EC}{\Delta t} f \quad (6)$$

Where f = 22.2 is a conversion factor of EC to urea hydrolysed (11.1) divided by the dilution factor (1:2) of initial urea concentration [55]. The slope and standard error of the measured changes in EC over time was computed through a linear regression with the data points of the three replicate runs.

2.9. Chemical analyses

2.9.1. pH

Solution pH was measured with a pH meter (Orion Star A215, Thermo Scientific) probe (Orion ROSS Ultra SM 103BNUWP, Thermo Scientific), calibrated to three points (pH = 4, 7 and 10, Orion Application Solution, Thermo Scientific).

2.9.2. Ammonium (NH_4^+)

NH_4^+ in solution was analysed with an ammonium cuvette test (100-1,800 mg/L NH_4-N, LCK502, Hach UK) and spectrophotometer (DR 1900, Hach UK) according to the manufacturer instructions.

2.9.3. Electrical conductivity

Solution EC was measured with an EC meter (Orion 5 Star, Thermo Scientific) probe (Orion 013605MD, Thermo Scientific) calibrated to 1413 and 12880 µS/cm buffer solutions (Orion Application Solution, Thermo Scientific).

2.9.4. Soil total carbon

COV14 soil total carbon and isotopic $\delta^{13}C$ composition were analysed with a Picarro Combustion Module Cavity Ring-Down Spectroscopy (CM-CRDS) system (CM by NC Technologies, G2201-i CDRS) interfaced by a Caddy Continuous Flow Interface (A2100) on five analytical replicates.

2.9.5. Soil total and exchangeable elemental composition

The total elemental composition COV14 soil was carried out through a triacid hotplate digestion at the Scottish University Environment Research Centre (SUERC, East Kilbride, G75 0QF, Scotland, UK) in triplicate. Soil samples were consecutively digested overnight on a hotplate at 120º, first with HF+HNO_3, secondly with HNO_3, and finally with HCl. Elements Al, Ba, Ca, Fe, K, Mg, Mn, Na, Sr, Ti and Zn were determined by inductively coupled plasma-optical emission spectrometry (ICP-OES, Thermo Scientific iCap 7000) and As, B, Cd, Co, Cr, Cu, Li, Mo, Ni, Pb, Sb, Sn and V by ICP-mass spectrometry (ICP-MS, Agilent 7500ce). ICP-MS was used due to the higher limit of detection over ICP-OES according to SUERC internal laboratory procedures.

The elemental composition of the soil exchangeable fraction was determined on three analytical replicates through the first step of the Tessier et al. (1979) sequential extraction. In summary, 1 g of soil and 8 mL of 1 M MgCl were mixed for 1 h at toom temperature. The solution containing soil exchangeable elements was obtained through centrifugation, decantation, filtration (0.2 µm), and acidification with HNO_3. Elements Na, K, Mg, Ca, Sr, Ba, Ti, V, Cr, Mo, Mn, Fe, Co, Ni, Cu, Zn, Cd, B, Al, Si, Sn, Pb, As, Sb, S, Se were determined by ICP-OES (Agilent 5900 SVDV).

2.9.6. Total dissolved organic carbon in soil extracts

The total dissolved organic carbon of the 1:2.5 COV14 soil extract was determined on three analytical replicates with a total organic carbon analyser (TOC-L, Shimadzu) calibrated to 2.5 and 5 ppm potassium phthalate monobasic (>99.5%, Sigma Aldrich).

3. Results and Discussion

3.2. Soil characterisation

The polluted COV14 soil was composed of 70% sand, 7.9±0.3% silt and 4.7±0.2% clay size-particles (Table S1). The moisture content was determined at 23%. The total carbon and isotopic composition of ^{13}C were 8±4% and -26.4 ‰±0.4, respectively (n =5) (Table S2). The soil total elemental analysis indicated Pb (490±30 mg/kg), Mn (460±50 mg/kg), Ba (470±50 mg/kg), Cu (240±90 mg/kg) and Zn (310±20 mg/kg) were present in significant concentrations (Figure S2A). Of these, only Mn (28±3 mg/kg) and Ba (10±3 mg/kg) were present at concentrations >5 mg/kg in the soil exchangeable fraction (Figure S2B). The analysis of soil PAH indicated presence of phenanthrene (28.7±0.2 mg/kg), fluoranthene (18.4±0.2 mg/kg) and pyrene (16.0±0.1 mg/kg). Additionally, anthracene, fluorene, benzo(a)anthracene, benzo(b)fluoranthene, acenaphthylene (5-10 mg/kg) and naphthalene, chrysene, benzo(k)fluoranthene, benzo(a)pyrene, indeno(1,2,3-cd)pyrene, dibenzo(a,h)anthracene and benzo(g,h,i)perylene were quantified (1-5 mg/kg) (Figure S3). These results confirmed presence of both organic and inorganic pollutants in COV14 soil.

3.3. Soil genetic potential for bioremediation

Bacterial ureC genes, relevant in the bioremediation of heavy metals through microbial-induced calcium carbonate precipitation, was evidenced in both the uncontaminated GQ soil and the PAH contaminated COV14 soil in extracted environmental DNA samples (Figure 1). The presence of ureC was confirmed by the amplification of a PCR product with the expected size of 318 bp[43] indicating the soils' potential for ureolysis. Of the ureC primers tested, the primer by Collier et al. [43] provided the best results, binding to the DNA ureC gene and ureC standard over a temperature range 50-61˚C (Figure S5Figure S 5). The ureC607F&898R pair[45] provided good results binding to DNA and ureC standard over 56-62˚C with strongest bands showing at 56˚C (Figure S7). The ureC 2LF&R primer[44] did not bind to DNA nor ureC standard at any of the annealing temperatures tested (56-68˚C) (Figure S6).

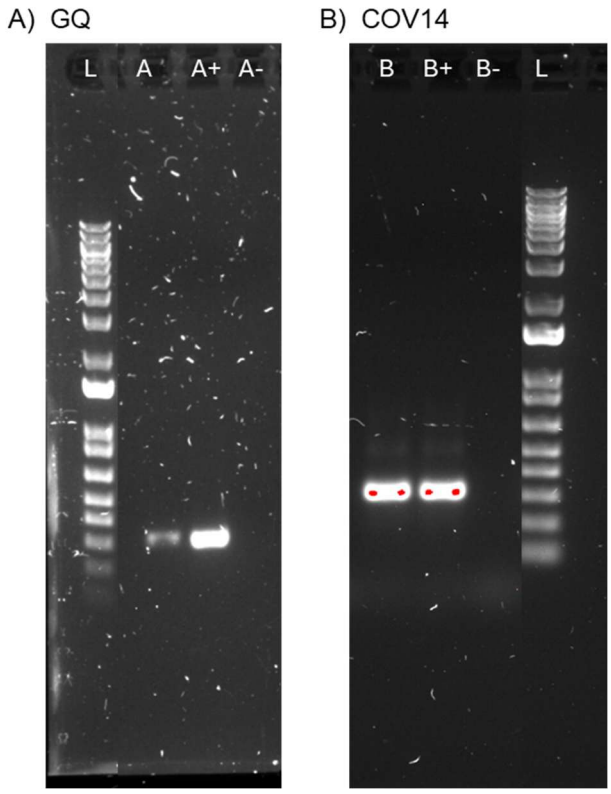

Figure 1 PCR results showing presence of ureC genes in DNA extracted from a) GQ and b) COV14 soil. Column well IDs without, with plus (+) and negative (-) signs indicate environmental DNA sample, environmental DNA sample spiked with 1 µL ureC standard and control PCR water, respectively. "L" stands for ladder used to estimate the base pair (bp) length of the target gene. ureC primers used developed by Collier et al., [43].

3.4. Ureolytic activity of autochthonous soil microorganisms

Biostimulation of urea hydrolysis in the uncontaminated quarry sand (GC) used as control was evidenced by increases in NH_4^+ (205±5 to 859±54 mM) and pH (6 to 9±0.01) within two days (Figure 2). The increase in NH_4^+ (ΔNH_4^+ = 654 mM) indicated all urea applied (333 mM) had been hydrolysed, according to the stoichiometry of the urea hydrolysis reaction (Eq.(1). Urea hydrolysis induces an increase in soil pH and NH_4^+ due to excess OH^- resulting from equilibration of CO_2 and NH_3 derived from urea hydrolysis with water (Eq. (2 and (3). This demonstrated a urease activity of 227 μM urea/min until consumption of all urea. The same treatment application to COV14 soil did not result in significant changes in pH (7.1-7.4) or NH_4^+ (205 mM) over 62 days (Figure 2), indicating urea hydrolysis in the polluted soil (COV14) did not occur to a measurable extent. Given the presence of ureC genes indicating COV14 soils' genetic potential for urea hydrolysis (Figure 1), the absence of urea hydrolysis soil could be attributed mainly to the presence of soil contaminants.

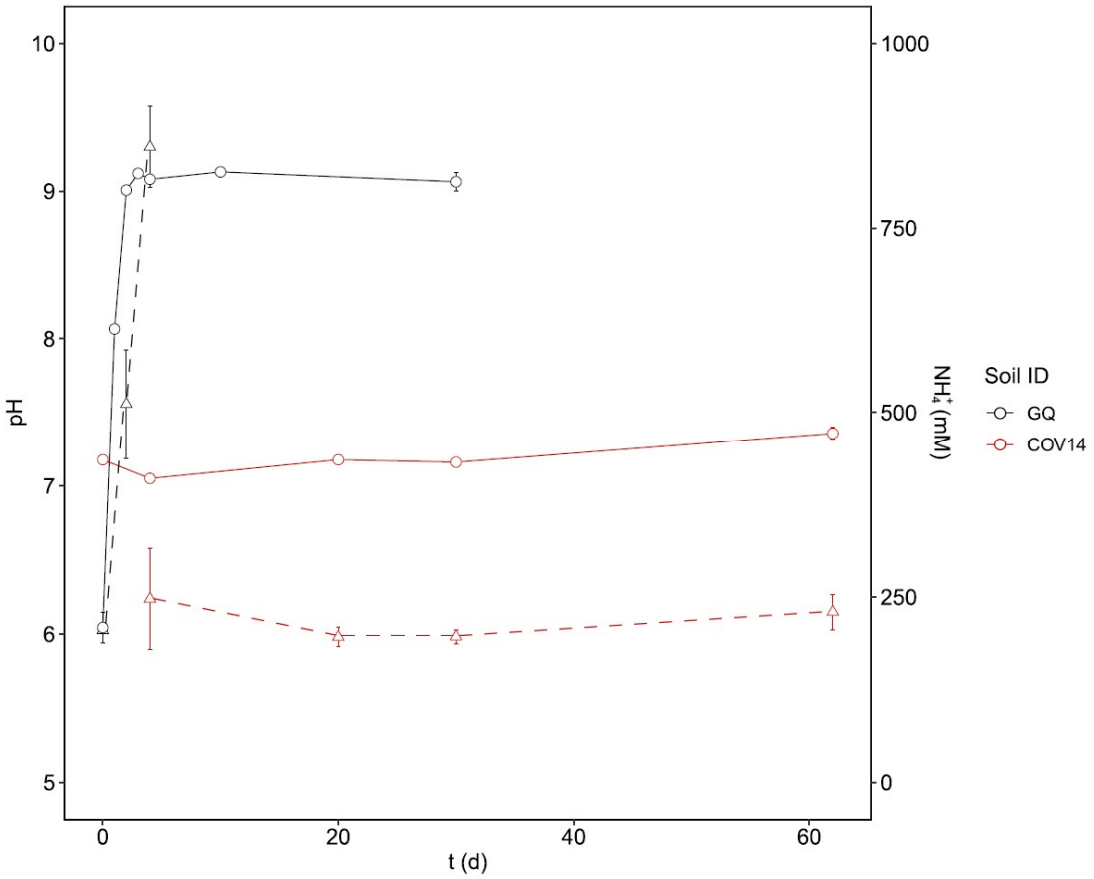

Figure 2 Evolution of soil pH (left y-axis, circle) and NH_4^+ (right y-axis, triangle) over time following application of treatment to induce urea hydrolysis on an uncontaminated quarry sand (GQ) and a polluted soil from a gas plant (COV14). Markers and error bars indicate the average and standard deviation of three replicate samples.

Heavy metals are known inhibitors of urea hydrolysis in soils. The strength of inhibition follows the order $Hg^{2+} \approx Ag^{+} > Cu^{2+} >> Ni^{2+} > Cd^{2+} > Zn^{2+} > Co^{2+} > Fe^{3+} > Pb^{2+} > Mn^{2+}$ [56; 57; 58]. The concentration of Mn and Ba in COV14 exchangeable fraction was determined at 28±3 and 10±3 mg/kg, respectively, equivalent to soil-solution concentrations of 0.5±0.1 and 0.07±0.02 mM. The rest of elements in the COV14 soil exchangeable fraction were <0.02 mM. Urea hydrolysis inhibition in pure cultures of *S. pasteurii* has been observed at Mn = 50 mM[59] although the minimum inhibitory concentration remains undetermined. For Ba, no data exist yet to our knowledge in pure cultures. Inhibitory concentrations of urea hydrolysis vary across elements and bacterial species however, studies on pure cultures indicate minimum inhibitory concentrations are typically one to three orders of magnitude higher than 0.02 mM [6; 60; 61, 62; 63]. Biostimulation of urea hydrolysis was not hindered in a soil containing Mn and Ba concentrations in the exchangeable fraction (10±1 and 33±1 mg/kg) similar to COV14[41]. It was therefore concluded that elements present in the exchangeable fraction at the concentrations determined were not the main cause of urea hydrolysis inhibition in COV14 soil.

Organic contaminants can have both stimulatory and inhibitory effects on soil urea hydrolysis. Increases in urease activity have been observed at PAH <2 mg/kg[27] and specifically <1 mg/kg naphthalene and phenanthrene[23], attributed to utilisation of organic contaminants as carbon sources by autochthonous microorganisms resulting in increased microbial counts, soil respiration, biomass, and enzyme activities[23]. On the contrary, sharp reductions in urease activity have been observed at total petroleum hydrocarbon (TPH) >300 mg/kg[28], and in the combined presence of PAH (phenanthrene, fluoranthene, benzo(a)pyrene; 0.01-3.2 mg/kg) and heavy metals (Cd, Zn, Pb)[30]. Inhibitory effects have been attributed to suppression of the microbial populations involved in the N, P, or C cycles[28], prevention of enzyme activity expression due to interaction of organic contaminants with cell surfaces[29] and changes in the enzyme molecular structure active site caused by heavy metal interactions and enzyme denaturation by PAH[30]. The measured PAH in COV14 added up to 116 mg/kg, an order of magnitude higher than PAH concentrations observed to decrease urea hydrolysis rates (PAH ~2 mg/kg)[27; 30]. Biostimulation of urea hydrolysis by COV14 soils' autochthonous bacteria was thus likely inhibited by the PAH.

3.5. Viability of *Sporosarcina pasteurii* in the presence of hydrocarbons

Hydrocarbon mediated inhibition of urea degradation may be the result of negative effects on bacteria growth and enzyme activity. To assess whether ureolytic bacteria could grow once introduced in the polluted soil environment, we used flow cytometry to quantify total and intact cell counts over the course of 24 hours and determine growth kinetics under increasing concentration of hydrocarbons.

The growth of *S. pasteurii* followed the typical bacteria growth pattern distinguished by a lag, exponential growth, stationary, and decline phases (Figure 3A). Surprisingly, the presence of hydrocarbons had no significant effect on the growth parameters compared to control (HC = 0; $p > 0.05$). The specific growth rates determined from the exponential phase of the total cell count remained consistent across hydrocarbon concentrations (ranging from 0.44 to 0.46 h^{-1}), except at the highest hydrocarbon concentration where a notable increase (HC 1 = 0.68±0.51 h^{-1}) determined (Figure 3C). Although this indicated a potential enhancement in growth, differences in specific growth rate were not statistically different ($p = 0.97$). Similarly, there were no significant differences in lag time in the presence of hydrocarbons compared to control for both intact ($p = 0.4$) and total ($p = 0.89$) cell count (Figure 3D). This demonstrated the bacteria's ability to acclimatise to the new environment was not affected by the presence of hydrocarbons and that bacteria were readily able to utilise the carbon sources in the media.

Hydrocarbons can be toxic to bacteria reducing the growth rate by causing membrane damage[64]. The total and intact cell counts after 24 hours (~$5x10^8$ cells/mL for total cell count, $p = 0.86$; ~$1.6x10^7$ cells/mL for intact cell count, $p = 0.89$) were not significantly different across samples (Figure 3A-B). Results further indicated that at least 2% of the total measured bacteria had an intact and undamaged cell membrane after 24 h. Added to the insignificant differences observed in lag and growth rate phases, it was concluded that *S. pasteurii* was able to grow successfully in the presence of hydrocarbons and there was no significant difference in bacteria numbers and cell viability after 24 h, regardless of presence of hydrocarbons at the concentrations tested.

Despite there being no significant increase in specific growth rate with increasing hydrocarbon concentration, *S. pasteurii* could be utilising additional carbon sources for growth. LBU media was constant across tested solutions, and the only difference was the organic carbon dissolved from soil during the water extraction procedure. It has been argued that PAH (phenanthrene, anthracene, fluoranthene, pyrene, benzo[a]anthracene and chrysene) can be easily used by the soil microorganisms as a source of carbon and energy[65; 66], were low toxicity, three-ring PAH, are decomposed more easily by microorganisms than five-ring PAH[67]. Notably, *Pseudomonas aeruginosa* N6P6, a known ureolytic bacteria, was able to utilise PAH as a sole source of carbon[68], indicating this could be a common trait across ureolytic bacteria. It is also possible that dissolved organic matter from the soil offered a protection mechanism. Higher soil organic matter was found to decrease the negative effects of PAH on soil urease activity[27, 69], which has been attributed to sorption of organic pollutants by soil organic matter[70; 71]. In this study we did not elucidate whether *S. pasteurii* used hydrocarbons, other dissolved organic carbon from soil or compounds in LBU media as source of carbon. However, the presence of only one lag and exponential phase indicated bacteria did not show a diauxic growth and therefore used one preferred carbon source[64].

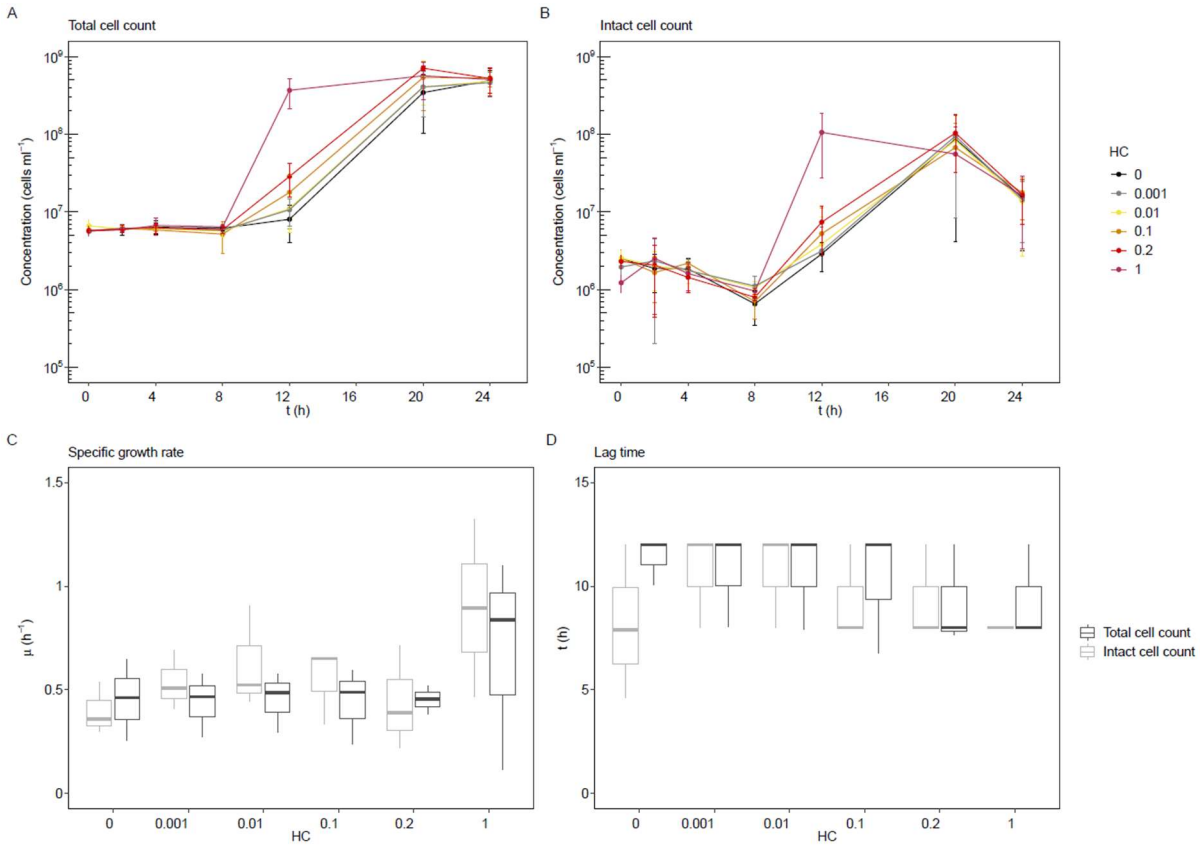

Figure 3 Growth curve and kinetics of *S. pasteurii* (cells/mL) population over 24 hours with different dilutions of hydrocarbon. Flow cytometry is used to measure the A) Total and B) Intact cell count. C) Growth rate (h^{-1}) and D) Lag time (h) of the intact and total cell count is calculated using the slope and intercept. Markers and error bars indicate the average and standard deviation of three biological replicate samples.

3.6. Urease activity of *Glycine Max* urease and *Sporosarcina pasteurii* in the presence of hydrocarbons

To establish whether organic contamination and PAH in particular inhibited urea hydrolysis, we investigated both the urease activity of *Glycine Max* and *S. pasteurii* in the presence of a COV14 water extract. The total organic carbon of the undiluted water soil extract (referred to as HC = 1) was determined at 70.0±0.7 mg/L (n = 3).

3.6.1. Urease activity in absence of contaminants

The urease activity of *Glycine Max* at 1 and 100 g bean/L in absence of contaminants was determined at 114±7 and 4521±304 µmol urea/min (HC = 0, Figure 4A) (Eq. (6) and the *S. pasteurii* urease activity at OD_{600} = 0.01 and 1 at 30±9.6 and 2102±26 µmol urea/min (HC = 0, Figure 5A), respectively. The urease activities at the higher dosages of enzyme (100 g bean/L) and cell (OD_{600} = 1) were comparable to values reported in the literature by Weng et al. [54] (~4.2 mM urea/min) and Minto et al. [53] (~3.7-4.6 mM urea/min/OD_{600}), respectively,

but significantly lower than values reported by Liu et al. [72] for *Glycine Max* (~10 mM urea/min) and Lauchnor et al., [73] for *S. pasteurii* (1.93 mM urea/min at OD_{600} = 0.025). The variation in urease activity of Glycine Max could arise from the grinding process (e.g., particle size of ground beans, inactivation of enzyme if temperature during grinding exceeded T >65°C Pettit et al. [74]) and the temperature at which EC conductivity is measured. Another cause for discrepancy at the higher dosages could be the lower urea concentration used in this study of 666 mM compared to the 1.1 M[55] which may have been insufficient to saturate the enzyme and prevented urease activity to reach v_{max}.

The measured urease activity of *S. pasteurii* was 2.0 to 3.7 times lower than that of *Glycine Max*. At equivalent amounts of enzyme, the reported urease activity of *S. pastuerii* is significantly higher than that of *Glycine Max* (2500 vs 650-800 µmol urea/min/mg enzyme, respectively)[38], indicating the amount of urease obtained with 1 and 100 g/L *Glycine Max* and OD_{600} = 0.01 and 1 *S. pasteurii* were not equivalent.

The measured urease activities of *Glycine Max* urease and *S. pasteurii* were not proportional to their respective concentrations. Instead of the x100 factor in urease activity expected from dilution, the difference in urease activity obtained with the lower and higher enzyme and cell dosages were x36 and x40, respectively. This was in contrast to the reported proportionality between urease activity and concentration of *Glycine Max* within 20-100 g/L[72] and *S. pasteurii* cell within OD_{600} = 0.025-0.15[73] and was attributed to insufficient urea to reach v_{max} at the higher dosages of enzyme and cell.

3.6.2. Effect of hydrocarbons on enzyme urease activity

At both 1 and 100 g/L *Glycine Max*, urease activity was quantifiable at all hydrocarbon concentrations (Figure 4A). At 100 g/L, no significant differences in urease activity were determined at any hydrocarbon concentration (p = 0.88) (Figure 4A). Instead, at 1 g/L urease activity decreased significantly with increasing hydrocarbon concentration (p = 4.24e-05) (Figure 4B), evidencing inhibition by hydrocarbons at enzyme level. A significant decrease in urease activity was determined at TOC ≥3.5±0.1 mg/L (i.e., HC ≥0.1)). At the highest hydrocarbon concentration (TOC = 35 mg/L, HC = 1), urease activity was 61% lower than in absence of contaminants (HC = 0). We do not know of any earlier studies on the effect of PAH on enzyme urease activity relevant for comparison with these results. Our results evidenced urease activity inhibition was dependant on enzyme and pollutant concentration. This suggested the mechanism of inhibition at enzyme level was competitive.

3.6.3. Effect of hydrocarbons on cell urease activity

Urease activity of *S. pasteurii* at OD_{600} = 1 was quantified at all hydrocarbon concentrations tested (Figure 5A). Presence of hydrocarbons had a significant effect on cell urease activity (p = 5.01e-05). A significant decrease in cell urease activity was determined at the lowest hydrocarbon concentration tested (HC ≥0.01, TOC = 0.7±0.1 mg/L, Figure 5A), resulting in a 31% slowdown in urease activity at the highest hydrocarbon concentration (HC = 1, TOC = 35 mg/L). The results at OD_{600} = 1 evidenced an inhibitory effect of hydrocarbons on cell urease activity. At OD_{600} = 0.01, cell urease activity was determined <60 µM/min at all hydrocarbon concentrations tested (Figure 5B). Changes in electrical conductivity over time at OD_{600} = 0.01 were hardly detectable over the 20 min experiment, resulting in linear regressions with slopes ranging from 0.6-1.6±0.03-0.48 µS/cm^2/min which were not significantly different than controls without cells (-1.8-2.2±0.2 µS/cm^2/min). Therefore, it was concluded that cell urease activity at OD_{600} = 0.01 was either below detection limits or was inhibited altogether, such that the effect of hydrocarbons on urease activity could not be elucidated. However, these results evidence cell urease activity inhibition was dependant on pollutant and cell concentration.

Contrary to the enzyme assay, inhibition was readily observed at the highest cell (OD_{600} = 1) and lowest contaminant concentration (TOC = 0.35 mg/L), suggesting PAH had a stronger inhibitory effect at cell than enzyme level. This could be because the amount of enzyme urease in *Glycine max* and *S. pasteurii* solutions were not equivalent, as indicated from urease activities obtained in absence of contaminants. Additionally, the *Glycine max* solution contained an undetermined amount of dissolved organic matter (<0.22 µm) which could bind to PAH[27, 75], decreasing its inhibitory effect. At the lowest cell concentration (OD_{600} = 0.01), no measurable urease activity was determined in presence or absence of contaminants indicating urease activity was below limits of detection. Future experiments with pure urease extract and equivalent and normalised urease enzyme concentrations would be necessary to elucidate differences in strength of inhibition at enzyme and cell level.

It has been suggested PAH have a non-specific narcotic mode of action on bacteria[34, 35]. This narcotic mode of action has been observed in soil nitrifiers, where nitrification rates decreased proportionally to PAHs' lipophilicity[36], suggesting cells might be exposed to a combined inhibitory effect occurring at cell and enzyme level. The urea hydrolysis assay revealed that cell (OD_{600} = 1, ~10^9 cells/ml; Figure 5) and enzyme (1 g/L, Figure 4) urease activity were significantly impeded with increasing hydrocarbon concentration, suggesting urea hydrolysis was largely inhibited at the low initial cell concentration used in the growth experiment (OD_{600} = 0.01, ~10^6 cells/ml) (Figure 3). The fact that the lag and exponential

growth phases did not show any significant differences across hydrocarbon concentrations thus indicated bacteria used carbon sources other than urea for growth. Furthermore, this indicated the negative effects on urease activity with increasing hydrocarbon concentration were due to negative effects on the enzyme urease rather than the overall cell function.

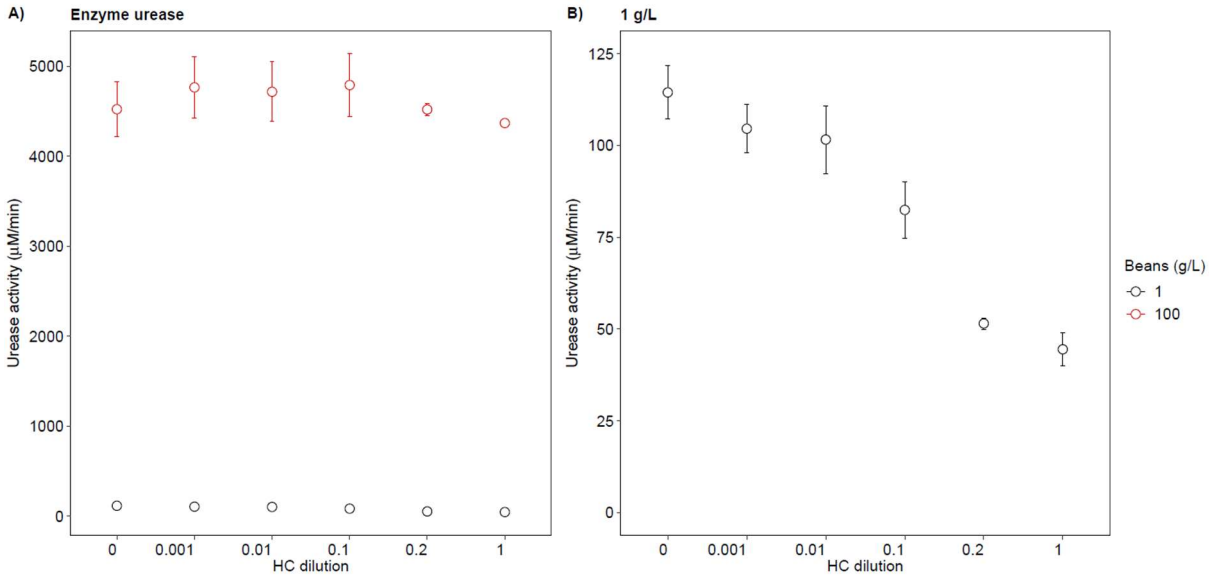

Figure 4 Urease activity of *Glycine Max* urease in presence of hydrocarbons (HC) extracted from soil COV-14. A) *Glycine Max* urease concentration of 1 and 100 g/L; B) *Glycine Max* urease concentration of 1 g/L. Markers and error bars indicate average and standard deviation of three replicate tests.

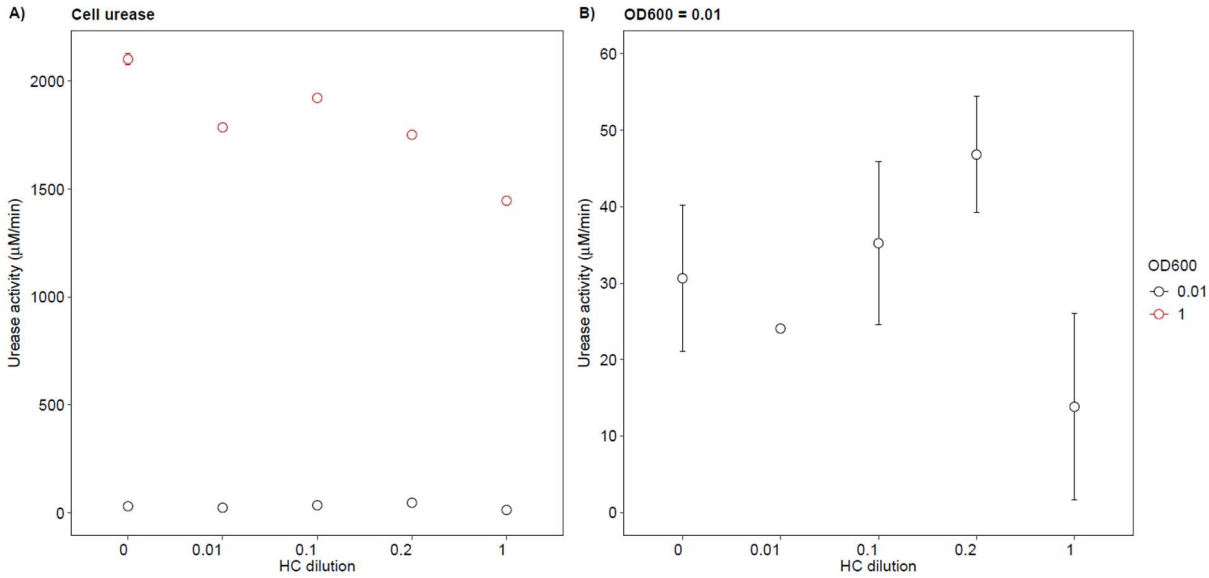

Figure 5 Urease activity of *S. pasteurii* in presence of hydrocarbons (HC) extracted from soil COV-14. A) *S. pasteurii* cell OD_{600} = 0.01 and 1; B) *S. pasteurii* cell OD_{600} = 0.01. Markers and error bars indicate average and standard deviation of three replicate tests.

3.7. Bioaugmentation of urea hydrolysis with *Sporosarcina pasteurii*

Based on the successful growth and urease activity of *S. pasteurii* in the COV14 soil extract containing hydrocarbons (Figure 3A and Figure 5), we conducted a bioaugmentation experiment in COV14 soil with *S. pasteurii* at OD_{600} = 1. Following inoculation of *S. pasteurii* and urea on COV14 soil, pH increased from 7.5 to 9 in the first 24 h and remained stable for 7 days. Similarly, NH_4^+ increased from 20±1 to 515±19 mM within the first day, remaining stable until the end of the experiment, equivalent to 77% urea hydrolysed. These results confirmed feasibility of urea hydrolysis by *S. pasteurii* in soil polluted by PAH via bioaugmentation.

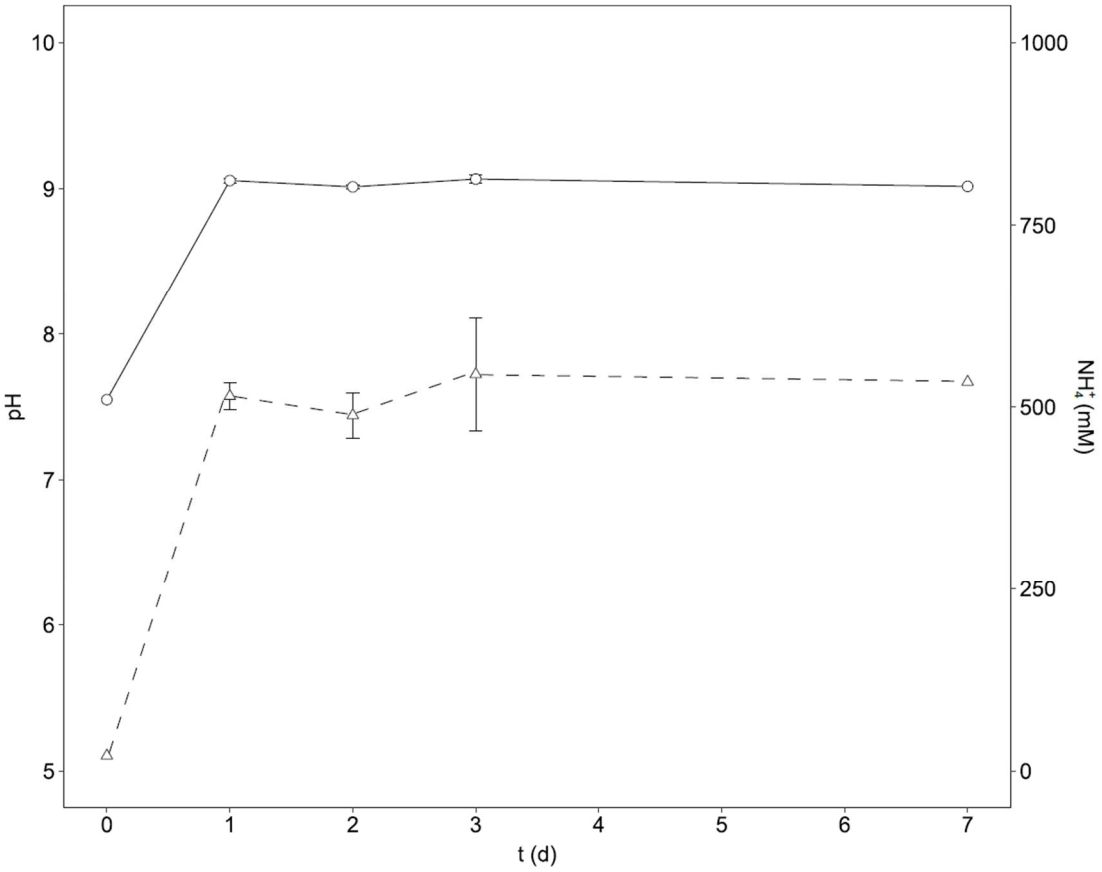

Figure 6 Evolution of soil pH (left y-axis, circle) and NH_4^+ (right y-axis, triangle) over time following bioaugmentation of *S. pasteurii* to induce urea hydrolysis in polluted soil from a gas plant (COV-14). Markers and error bars indicate the average and standard deviation of three replicate samples.

Acknowledgments

This work has been conducted as part of the GALLANT project and is funded by the Natural Environment Research Council as part of the Changing the Environment Programme [grant number NE/W005042/1]. Special thanks are given to the funding body UKRI Natural

Environment Research Council, to A. Hunter, E. Palmer, Dr C. Brolly, K. Roberts of the University of Glasgow for their technical support, to Dr V. Olive and Dr G. MacKinnon of the Scottish Universities Environmental Research Centre (SUERC) for the expert advice and analysis of samples, to E. Murray of the GALLANT research project for the administrative support, and to Dr G. El Mountassir of Strathclyde University and J. Fraser of Hugh King Tillicoultry Quarries for sourcing materials.

References

[1] FAO and UNEP. 2021. *Global Assessment of Soil Pollution: Report.* Rome. https://doi.org/10.4060/cb4894en.

[2] Chai, L., Huang, S., Yang, Z., Peng, B., Huang, Y., Chen, Y., 2009. Cr (VI) remediation by indigenous bacteria in soils contaminated by chromium containing slag. J Hazard Mater 167 (1-3), 516–522. https://doi.org/10.1016/j.jhazmat.2009.01.030.

[3] Achal, V., Pan, X., Lee, D.J., Kumari, D., Zhang, D., 2013. Remediation of Cr(VI) from chromium slag by biocementation. Chemosphere 93 (7), 1352–1358. https://doi.org/10.1016/j.chemosphere.2013.08.008.

[4] Kumari, D., Li, M., Pan, X., Xin-Yi, Q., 2014. Effect of bacterial treatment on Cr(VI) remediation from soil and subsequent plantation of Pisum sativum. Ecol Eng 73, 404–408. https://doi.org/10.1016/j.ecoleng.2014.09.093.

[5] Achal, V., Pan, X., Zhang, D., Fu, Q., 2012a. Bioremediation of Pb-contaminated soil based on microbially induced calcite precipitation. J Microbiol Biotechnol 22(2), 244–247. https://doi.org/10.4014/jmb.1108.08033.

[6] Govarthanan, M., Lee, K.J., Cho, M., Kim, J.S., Kamala-Kannan, S. and Oh, B.T., 2013. Significance of autochthonous Bacillus sp. KK1 on biomineralization of lead in mine tailings. *Chemosphere*, *90*(8), pp.2267-2272.

[7] Achal, V., Pan, X., Zhang, D., 2012b. Bioremediation of strontium (Sr) contaminated aquifer quartz sand based on carbonate precipitation induced by Sr resistant Halomonas sp. Chemosphere 89 (6), 764–768. https://doi.org/10.1016/j.chemosphere.2012.06.064.

[8] Yang, J., Pan, X., Zhao, C., Mou, S., Achal, V., Al-Misned, F.A., Mortuza, M.G., Gadd, G.M., 2016. Bioimmobilization of heavy metals in acidic copper mine tailings soil. Geomicrobiol J 33 (3-4), 261–266. https://doi.org/10.1080/01490451.2015.1068889.

[9] Liu, P., Zhang, Y., Tang, Q., Shi, S., 2021. Bioremediation of metal-contaminated soils by microbially-induced carbonate precipitation and its effects on ecotoxicity and long-term stability. Biochem Eng J 166, 107856. https://doi.org/10.1016/j.bej.2020.107856.

[10] Achal, V., Pan, X., Fu, Q., Zhang, D., 2012. Biomineralization based remediation of As (III) contaminated soil by Sporosarcina ginsengisoli. J Hazard Mater 201,178‐184. https://doi.org/10.1016/j.jhazmat.2011.11.067.

[11] Zhu, X., Li, W., Zhan, L., Huang, M., Zhang, Q., Achal, V., 2016. The large-scale process of microbial carbonate precipitation for nickel remediation from an industrial soil. Environ Pollut 219, 149‐155. https://doi.org/10.1016/j.envpol.2016.10.047.

[12] Chen, X., Achal, V., 2019. Biostimulation of carbonate precipitation process in soil for copper immobilization. J Hazard Mater 368, 705‐713. https://doi.org/10.1016/j.jhazmat.2019.01.108.

[13] Li, Y.F., Hao, S., Ma, W.L., Yang, P.F., Li, W.L., Zhang, Z.F., Liu, L.Y. and Macdonald, R.W., 2024. Persistent organic pollutants in global surface soils: distributions and fractionations. Environmental Science and Ecotechnology, 18, p.100311.

[14] Heywood, E., Wright, J., Wienburg, C.L., Black, H.I., Long, S.M., Osborn, D. and Spurgeon, D.J., 2006. Factors influencing the national distribution of polycyclic aromatic hydrocarbons and polychlorinated biphenyls in British soils. Environmental Science & Technology, 40(24), pp.7629-7635.

[15] Ye, S., Zeng, G., Wu, H., Zhang, C., Liang, J., Dai, J., Liu, Z., Xiong, W., Wan, J., Xu, P. and Cheng, M., 2017. Co-occurrence and interactions of pollutants, and their impacts on soil remediation—a review. Critical reviews in environmental science and technology, 47(16), pp.1528-1553.

[16] Dejong, J.T., Soga, K., Kavazanjian, E., Burns, S., Van Paassen, L.A., Al Qabany, A., Aydilek, A., Bang, S.S., Burbank, M., Caslake, L.F. and Chen, C.Y., 2014. Biogeochemical processes and geotechnical applications: progress, opportunities and challenges. In *Bio-and chemo-mechanical processes in geotechnical engineering: géotechnique symposium in print 2013* (pp. 143-157). Ice Publishing. https://doi.org/10.1680/bcmpge.60531.014.

[17] Burbank, M.B., Weaver, T.J., Williams, B.C., Crawford, R.L., 2012. Urease activity of ureolytic bacteria isolated from six soils in which calcite was precipitated by indigenous bacteria. Geomicrobiol J 29 (4), 389‐395. https://doi.org/10.1080/01490451.2011.575913.

[18] Mitchell, J.K. and Santamarina, J.C., 2005. Biological considerations in geotechnical engineering. *Journal of geotechnical and geoenvironmental engineering*, *131*(10), pp.1222-1233. https://doi.org/10.1061/(ASCE)1090-0241(2005)131:10(1222).

[19] Mortensen, B.M., Haber, M.J., DeJong, J.T., Caslake, L.F. and Nelson, D.C., 2011. Effects of environmental factors on microbial induced calcium carbonate precipitation. *Journal of applied microbiology*, *111*(2), pp.338-349. https://doi.org/10.1111/j.1365-2672.2011.05065.x.

[20] Stabnikov, V., Jian, C., Ivanov, V. and Li, Y., 2013. Halotolerant, alkaliphilic urease-producing bacteria from different climate zones and their application for biocementation of sand. *World Journal of Microbiology and Biotechnology*, *29*, pp.1453-1460. https://doi.org/10.1007/s11274-013-1309-1.

[21] Cheng, L., Shahin, M.A., Cord-Ruwisch, R., Addis, M., Hartanto, T. and Elms, C., 2014, November. Soil stabilisation by microbial-induced calcite precipitation (MICP): investigation into some physical and environmental aspects. In *7th international congress on environmental geotechnics* (Vol. 64, No. 12, pp. 1105-1112). Engineers Australia Melbourne, Australia.

[22] Gat, D., Ronen, Z., Tsesarsky, M., 2017. Long-term sustainability of microbial induced CaCO3 precipitation in aqueous media. Chemosphere 184, 524–531. https://doi.org/10.1016/j.chemosphere.2017.06.015.

[23] Margesin, R., Walder, G., Schinner, F., 2000a. The impact of hydrocarbon remediation (diesel oil and polycyclic aromatic hydrocarbons) on enzyme activities and microbial properties of soil. Acta Biotechnol. 20, 313– 333. https://doi.org/10.1002/abio.370200312.

[24] Margesin, R., Zimmerbauer, A. and Schinner, F., 2000b. Monitoring of bioremediation by soil biological activities. Chemosphere, 40(4), pp.339-346. https://doi.org/10.1016/S0045-6535(99)00218-0.

[25] Trasar-Cepeda, C., Leiros, M.C., Seoane, S. and Gil-Sotres, F., 2000. Limitations of soil enzymes as indicators of soil pollution. *Soil Biology and Biochemistry*, *32*(13), pp.1867-1875. https://doi.org/10.1016/S0038-0717(00)00160-7.

[26] Dindar, E., Şağban, F.O.T. and Başkaya, H.S., 2015. Variations of soil enzyme activities in petroleum-hydrocarbon contaminated soil. International Biodeterioration & Biodegradation, 105, pp.268-275. https://doi.org/10.1016/j.ibiod.2015.09.011.

[27] Baran, S., Bielińska, J.E. and Oleszczuk, P., 2004. Enzymatic activity in an airfield soil polluted with polycyclic aromatic hydrocarbons. Geoderma, 118(3-4), pp.221-232. https://doi.org/10.1016/S0016-7061(03)00205-2.

[28] Guo, H., Yao, J., Cai, M., Qian, Y., Guo, Y., Richnow, H.H., Blake, R.E., Doni, S. and Ceccanti, B., 2012. Effects of petroleum contamination on soil microbial numbers, metabolic activity and urease activity. Chemosphere, 87(11), pp.1273-1280. https://doi.org/10.1016/j.chemosphere.2012.01.034.

[29] Andreoni, V., Cavalca, L., Rao, M.A., Nocerino, G., Bernasconi, S., Dell'Amico, E., Colombo, M. and Gianfreda, L., 2004. Bacterial communities and enzyme activities of PAHs polluted soils. *Chemosphere*, *57*(5), pp.401-412. https://doi.org/10.1016/j.chemosphere.2004.06.013.

[30] Shen, G., Lu, Y. and Hong, J., 2006. Combined effect of heavy metals and polycyclic aromatic hydrocarbons on urease activity in soil. Ecotoxicology and Environmental Safety, 63(3), pp.474-480. https://doi.org/10.1016/j.ecoenv.2005.01.009.

[31] Wyszkowska, J. and Wyszkowski, M., 2010. Activity of soil dehydrogenases, urease, and acid and alkaline phosphatases in soil polluted with petroleum. *Journal of Toxicology and Environmental Health, Part A*, *73*(17-18), pp.1202-1210. https://doi.org/10.1080/15287394.2010.492004.

[32] Wu, B., Lan, T., Lu, D. and Liu, Z., 2014. Ecological and enzymatic responses to petroleum contamination. *Environmental Science: Processes & Impacts*, *16*(6), pp.1501-1509. https://doi.org/10.1039/C3EM00731F.

[33] Feyzi, H., Chorom, M. and Bagheri, G., 2020. Urease activity and microbial biomass of carbon in hydrocarbon contaminated soils. A case study of cheshmeh-khosh oil field, Iran. *Ecotoxicology and environmental safety*, *199*, p.110664. https://doi.org/10.1016/j.ecoenv.2020.110664.

[34] Moore, M.N., 1985. Cellular responses to pollutants. *Marine Pollution Bulletin*, *16*(4), pp.134-139. https://doi.org/10.1016/0025-326X(85)90003-7.

[35] Moore, M.N. and Farrar, S.V., 1985. Effects of polynuclear aromatic hydrocarbons on lysosomal membranes in molluscs. *Marine Environmental Research*, *17*(2-4), pp.222-225. https://doi.org/10.1016/0141-1136(85)90091-1.

[36] Sverdrup, L.E., Nielsen, T. and Krogh, P.H., 2002. Soil ecotoxicity of polycyclic aromatic hydrocarbons in relation to soil sorption, lipophilicity, and water solubility. *Environmental science & technology*, *36*(11), pp.2429-2435. https://doi.org/10.1021/es010180s.

[37] Liu, Y., Dai, Q., Jin, X., Dong, X., Peng, J., Wu, M., Liang, N., Pan, B. and Xing, B., 2018. Negative impacts of biochars on urease activity: high pH, heavy metals, polycyclic aromatic hydrocarbons, or free radicals?. *Environmental science & technology*, *52*(21), pp.12740-12747. https://doi.org/10.1021/acs.est.8b00672.

[38] Krajewska, B., 2009. Ureases I. Functional, catalytic and kinetic properties: A review. *Journal of molecular catalysis B: Enzymatic*, *59*(1-3), pp.9-21. https://doi.org/10.1016/j.molcatb.2009.01.003.

[40] Gauchotte-Lindsay, C., Aspray, T.J., Knapp, M. and Ijaz, U.Z., 2019. Systems biology approach to elucidation of contaminant biodegradation in complex samples–integration of high-resolution analytical and molecular tools. *Faraday discussions*, *218*, pp.481-504. https://doi.org/10.1039/C9FD00020H.

[41] Comadran-Casas, C., Unluer, C., Bass, A.M., Macdonald, J., Najafi, E.K., Spruzeniece, L. and Gauchotte-Lindsay, C., 2025. Bioremediation of multiple heavy metals through biostimulation of microbial-induced calcite precipitation at varying calcium-to-urea concentrations. *Journal of Hazardous Materials*, *491*, p.137691. https://doi.org/10.1016/j.jhazmat.2025.137691.

[42] Lee, L.S., Rao, P.S.C. and Okuda, I., 1992. Equilibrium partitioning of polycyclic aromatic hydrocarbons from coal tar into water. Environmental science & technology, 26(11), pp.2110-2115.

[43] Collier, J.L., Brahamsha, B. and Palenik, B., 1999. The marine cyanobacterium Synechococcus sp. WH7805 requires urease (urea amiohydrolase, EC 3.5. 1.5) to utilize urea as a nitrogen source: molecular-genetic and biochemical analysis of the enzyme. *Microbiology*, *145*(2), pp.447-459. https://doi.org/10.1099/13500872-145-2-447.

[44] Gresham, T.L., Sheridan, P.P., Watwood, M.E., Fujita, Y. and Colwell, F.S., 2007. Design and validation of ure C-based primers for groundwater detection of urea-hydrolyzing bacteria. *Geomicrobiology Journal*, *24*(3-4), pp.353-364. https://doi.org/10.1080/01490450701459283.

[45] Wang, Z., Feng, K., Wei, Z., Wu, Y., Isobe, K., Senoo, K., Peng, X., Wang, D., He, Q., Du, X. and Li, S., 2022. Evaluation and redesign of the primers for detecting nitrogen cycling genes in environments. *Methods in Ecology and Evolution*, *13*(9), pp.1976-1989. https://doi.org/10.1111/2041-210X.13946.

[46] Li, X., Manuel, J., Slavens, S., Crunkleton, D.W. and Johannes, T.W., 2021. Interactive effects of light quality and culturing temperature on algal cell size, biomass doubling time,

protein content, and carbohydrate content. *Applied Microbiology and Biotechnology*, *105*, pp.587-597. https://doi.org/10.1007/s00253-020-11068-y.

[47] Rolfe, M.D., Rice, C.J., Lucchini, S., Pin, C., Thompson, A., Cameron, A.D., Alston, M., Stringer, M.F., Betts, R.P., Baranyi, J. and Peck, M.W., 2012. Lag phase is a distinct growth phase that prepares bacteria for exponential growth and involves transient metal accumulation. *Journal of bacteriology*, *194*(3), pp.686-701. https://doi.org/10.1128/jb.06112-11.

[48] Myers, J.A., Curtis, B.S. and Curtis, W.R., 2013. Improving accuracy of cell and chromophore concentration measurements using optical density. *BMC biophysics*, *6*, pp.1-16. https://doi.org/10.1186/2046-1682-6-4

[49] Falcioni, T., Papa, S. and Gasol, J.M., 2008. Evaluating the flow-cytometric nucleic acid double-staining protocol in realistic situations of planktonic bacterial death. *Applied and environmental microbiology*, *74*(6), pp.1767-1779. https://doi.org/10.1128/AEM.01668-07.

[50] Nielsen, J.L., Kragelund, C. and Nielsen, P.H., 2009. Combination of fluorescence in situ hybridization with staining techniques for cell viability and accumulation of PHA and polyP in microorganisms in complex microbial systems. In *Bioremediation: Methods and Protocols* (pp. 103-116). Totowa, NJ: Humana Press.

[51] Vignola, M., Werner, D., Hammes, F., King, L.C. and Davenport, R.J., 2018. Flow-cytometric quantification of microbial cells on sand from water biofilters. *Water Research*, *143*, pp.66-76. https://doi.org/10.1016/j.watres.2018.05.053.

[52] Hall, B.G., Acar, H., Nandipati, A. and Barlow, M., 2014. Growth rates made easy. *Molecular biology and evolution*, *31*(1), pp.232-238. https://doi.org/10.1093/molbev/mst187.

[53] Minto, J.M., Tan, Q., Lunn, R.J., El Mountassir, G., Guo, H. and Cheng, X., 2018. 'Microbial mortar'-restoration of degraded marble structures with microbially induced carbonate precipitation. *Construction and Building Materials*, *180*, pp.44-54. https://doi.org/10.1016/j.conbuildmat.2018.05.200.

[54] Weng, Y., Lai, H., Zheng, J., Cui, M., Chen, Y., Xu, Z., Jiang, W., Zhang, J., & Song, Y. (2024). Effect of acid type on biomineralization of soil using crude soybean urease solution. Journal of Rock Mechanics and Geotechnical Engineering, 16(12), 5135-5146. https://doi.org/10.1016/j.jrmge.2024.09.017

[55] Whiffin, V.S., 2004. Microbial CaCO3 precipitation for the production of biocement (Doctoral dissertation, Murdoch University).

[56] Tabatabai, M.A., 1977. Effects of trace elements on urease activity in soils. *Soil biology and Biochemistry*, *9*(1), pp.9-13. https://doi.org/10.1016/0038-0717(77)90054-2.

[57] Krajewska, B., 1991. Urease immobilized on chitosan membrane. Inactivation by heavy metal ions. Journal of Chemical Technology & Biotechnology, 52(2), pp.157-162. https://doi.org/10.1002/jctb.280520203.

[58] Zaborska, W., Krajewska, B. and Olech, Z., 2004. Heavy metal ions inhibition of jack bean urease: potential for rapid contaminant probing. *Journal of Enzyme Inhibition and Medicinal Chemistry*, *19*(1), pp.65-69. https://doi.org/10.1080/14756360310001650237.

[59] Fang, L., Niu, Q., Cheng, L., Jiang, J., Yu, Y.Y., Chu, J., Achal, V. and You, T., 2021. Ca-mediated alleviation of Cd2+ induced toxicity and improved Cd2+ biomineralization by Sporosarcina pasteurii. *Science of The Total Environment*, *787*, p.147627. https://doi.org/10.1016/j.scitotenv.2021.147627.

[60] Mugwar, A.J. and Harbottle, M.J., 2016. Toxicity effects on metal sequestration by microbially-induced carbonate precipitation. *Journal of Hazardous Materials*, *314*, pp.237-248. https://doi.org/10.1016/j.jhazmat.2016.04.039.

[61] Jiang, N.J., Liu, R., Du, Y.J. and Bi, Y.Z., 2019. Microbial induced carbonate precipitation for immobilizing Pb contaminants: Toxic effects on bacterial activity and immobilization efficiency. *Science of the Total Environment*, *672*, pp.722-731. https://doi.org/10.1016/j.scitotenv.2019.03.294.

[62] Kang, C.H., Oh, S.J., Shin, Y., Han, S.H., Nam, I.H. and So, J.S., 2015. Bioremediation of lead by ureolytic bacteria isolated from soil at abandoned metal mines in South Korea. *Ecological Engineering*, *74*, pp.402-407. https://doi.org/10.1016/j.ecoleng.2014.10.009.

[63] Qiao, S., Zeng, G., Wang, X., Dai, C., Sheng, M., Chen, Q., Xu, F. and Xu, H., 2021. Multiple heavy metals immobilization based on microbially induced carbonate precipitation by ureolytic bacteria and the precipitation patterns exploration. *Chemosphere*, *274*, p.129661. https://doi.org/10.1016/j.chemosphere.2021.129661.

[64] Sikkema, J.A.N., de Bont, J.A. and Poolman, B., 1995. Mechanisms of membrane toxicity of hydrocarbons. Microbiological reviews, 59(2), pp.201-222. https://doi.org/10.1128/mr.59.2.201-222.1995.

[65] Cerniglia, C.E., 1984. Microbial metabolism of polycyclic aromatic hydrocarbons. *Advances in applied microbiology*, *30*, pp.31-71. https://doi.org/10.1016/S0065-2164(08)70052-2.

[66] Kanaly, R.A. and Harayama, S., 2000. Biodegradation of high-molecular-weight polycyclic aromatic hydrocarbons by bacteria. *Journal of bacteriology*, *182*(8), pp.2059-2067. https://doi.org/10.1128/jb.182.8.2059-2067.2000.

[67] Boonchan, S., Britz, M.L. and Stanley, G.A., 2000. Degradation and mineralization of high-molecular-weight polycyclic aromatic hydrocarbons by defined fungal-bacterial cocultures. *Applied and environmental microbiology*, *66*(3), pp.1007-1019. https://doi.org/10.1128/AEM.66.3.1007-1019.2000.

[68] Mangwani, N., Kumari, S. and Das, S., 2015. Involvement of quorum sensing genes in biofilm development and degradation of polycyclic aromatic hydrocarbons by a marine bacterium Pseudomonas aeruginosa N6P6. *Applied Microbiology and Biotechnology*, *99*, pp.10283-10297. https://doi.org/10.1007/s00253-015-6868-7.

[69] Lipińska, A., Kucharski, J. and Wyszkowska, J., 2013. Urease activity in soil contaminated with polycyclic aromatic hydrocarbons. Polish Journal of Environmental Studies, 22(5).

[70] Murphy, E.M., Zachara, J.M. and Smith, S.C., 1990. Influence of mineral-bound humic substances on the sorption of hydrophobic organic compounds. Environmental science & technology, 24(10), pp.1507-1516.

[71] Pignatello, J.J. and Xing, B., 1995. Mechanisms of slow sorption of organic chemicals to natural particles. Environmental science & technology, 30(1), pp.1-11. https://doi.org/10.1021/es940683g.

[72] Liu, L., Gao, Y., Geng, W., Song, J., Zhou, Y. and Li, C., 2023. Comparison of jack bean and soybean crude ureases on surface stabilization of desert sand via enzyme-induced carbonate precipitation. *Geoderma*, *435*, p.116504. https://doi.org/10.1016/j.geoderma.2023.116504.

[73] Lauchnor, E.G., Topp, D.M., Parker, A.E. and Gerlach, R., 2015. Whole cell kinetics of ureolysis by Sporosarcina pasteurii. *Journal of applied microbiology*, *118*(6), pp.1321-1332. https://doi.org/10.1111/jam.12804.

[74] Pettit, N.M., Smith, A.R.J., Freedman, R.B. and Burns, R.G., 1976. Soil urease: activity, stability and kinetic properties. *Soil Biology and Biochemistry*, *8*(6), pp.479-484. https://doi.org/10.1016/0038-0717(76)90089-4.

[75] Ukalska-Jaruga, A. and Smreczak, B., 2020. The impact of organic matter on polycyclic aromatic hydrocarbon (PAH) availability and persistence in soils. Molecules, 25(11), p.2470. https://doi.org/10.3390/molecules25112470.

Supplementary material

1. Soil characterisation

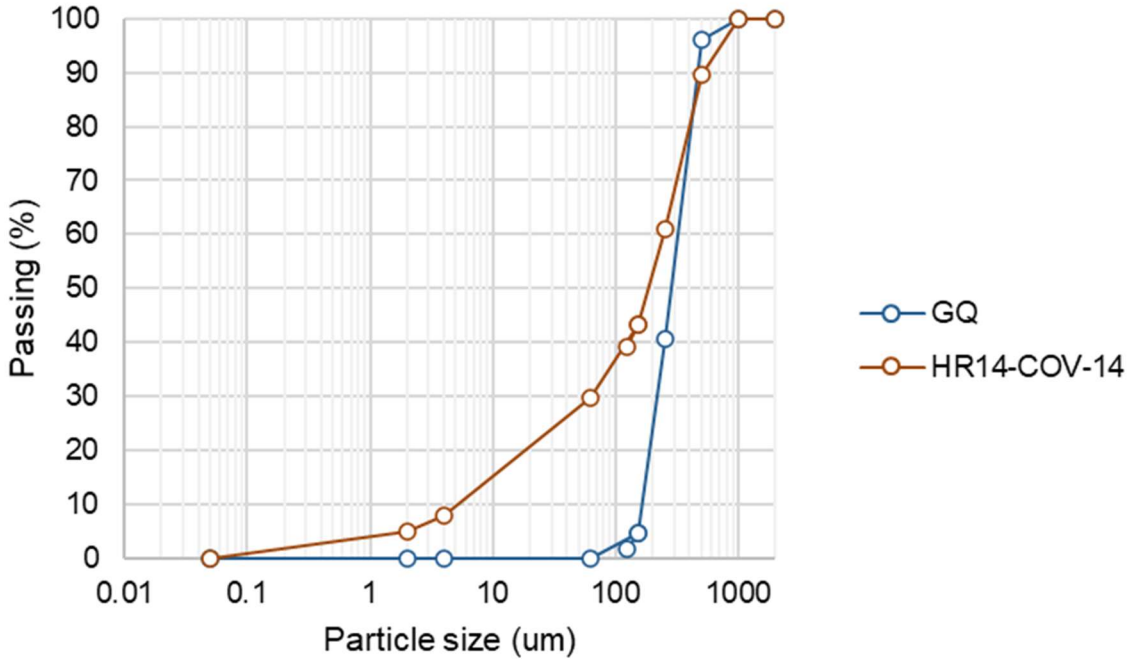

Figure S 1 Particle size distribution curves of quarry sand (GQ) and polluted soil (COV14) determined by laser diffraction on three replicates of <2 mm soil fractions.

Table S 1 Analysis of particle size distribution curves from Figure S 1.

Sample ID	Sand (1000-63 um)	Silt (63-2 um)	Clay (<2 um)	Cu	Cc
GQ	100	0	0	1.72	0.98
HR14-COV-14	70.35	24.92	4.7	42.96	3.04

Table S 2 COV14 Soil total carbon and isotopic δ13C composition analysed with a Picarro Combustion Module Cavity Ring-Down Spectroscopy (CM-CRDS) system (CM by NC Technologies, G2201-i CDRS) interfaced by a Caddy Continuous Flow Interface (A2100) on five analytical replicates.

Sample ID	weight (mg)	C measured (mg)	**d13C-corrected**	**Wt%-C (g/100g)**	dry weight (mg)	**Wt%-C (g/100g)**
COV-14/1	3.28	0.16	**-26.6**	**4.9**	2.53	6.341984
COV-14/2	6.03	0.21	**-26.2**	**3.4**	4.64	4.478789
COV-14/3	4.42	0.22	**-25.8**	**4.9**	3.40	6.385915
COV-14/4	3.19	0.18	**-26.7**	**5.7**	2.46	7.40655

COV-14/5	2.57	0.28	**-26.7**	**11.0**	1.98	14.3195

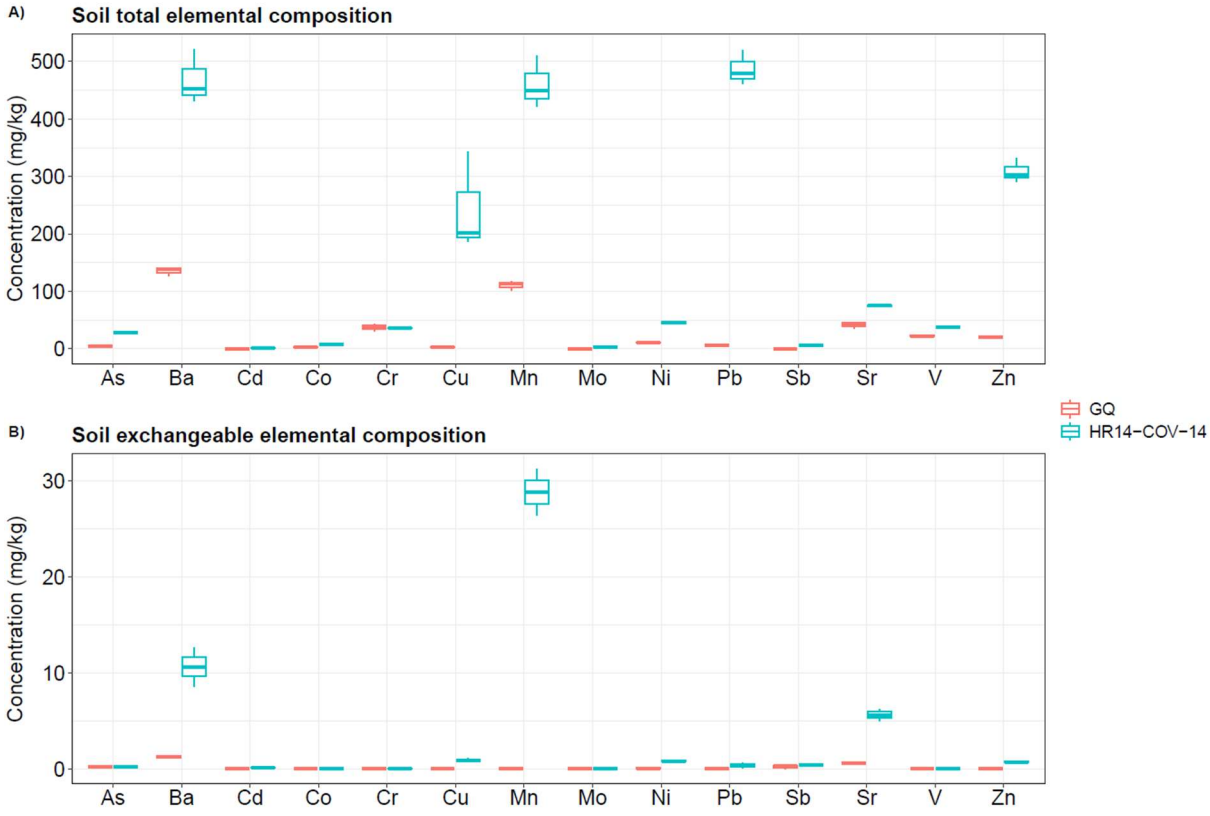

Figure S 2 Total (A) and exchangeable (B) elemental composition of GQ and COV14 soils (n = 3) determined by total soil digestion and step 1 of Tessier et al., (1979) sequential extraction, respectively, and analysed by ICP-OES/MS.

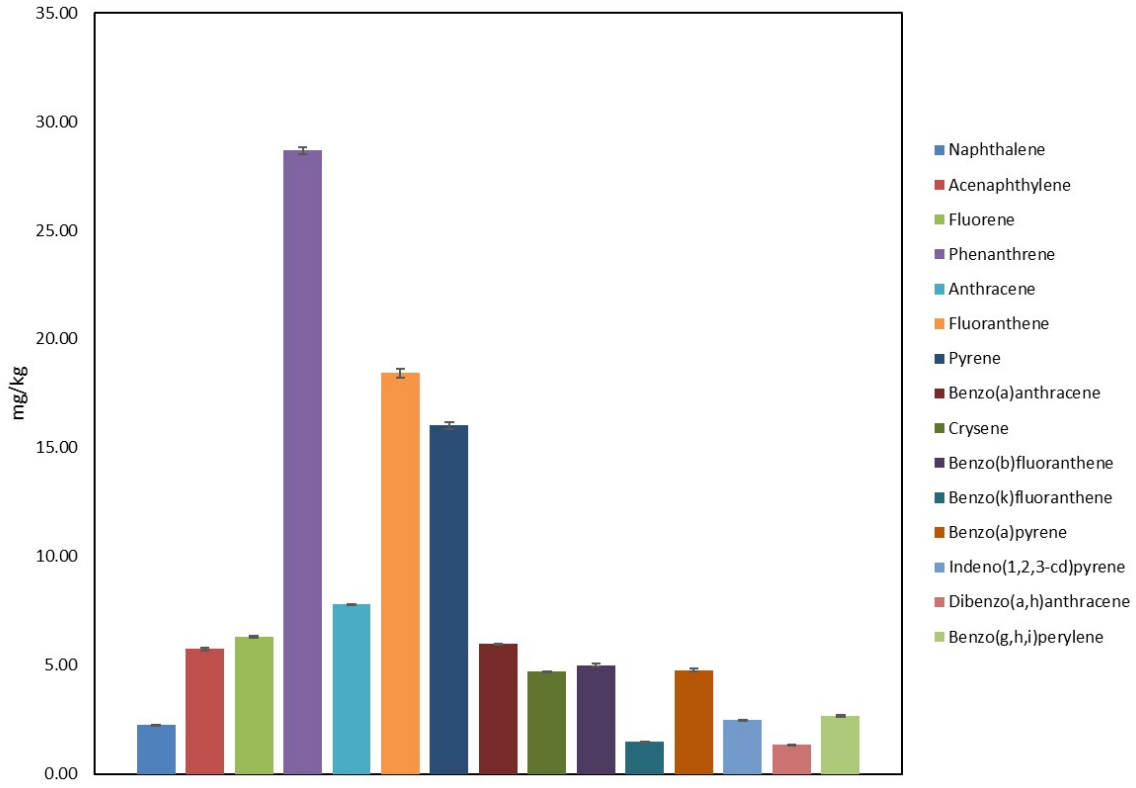

Figure S 3 Polycyclic aromatic hydrocarbon (PAH) concentrations of soil COV14 (n = 3).

2. ureC primer optimisation

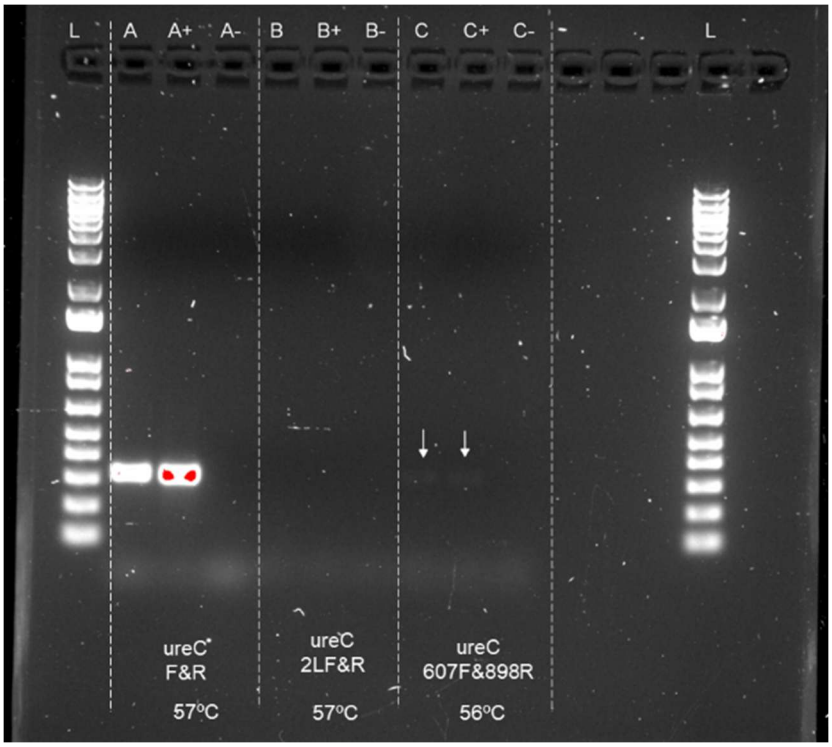

Figure S 4 PCR of ureC primers (ureC F&R, ureC 2LF&R and ureC 607F&898R) in environmental soil DNA tested at optimal annealing temperatures identified by Collier et al. (1999), Gresham et al. (2007) and

Wang et al. (2022), respectively. Column well IDs without, with plus (+) and negative (-) signs indicate environmental DNA sample, environmental DNA sample spiked with 1 µL ureC standard and control PCR water, respectively. "L" stands for ladder used to estimate the base pair (bp) length of the target gene.

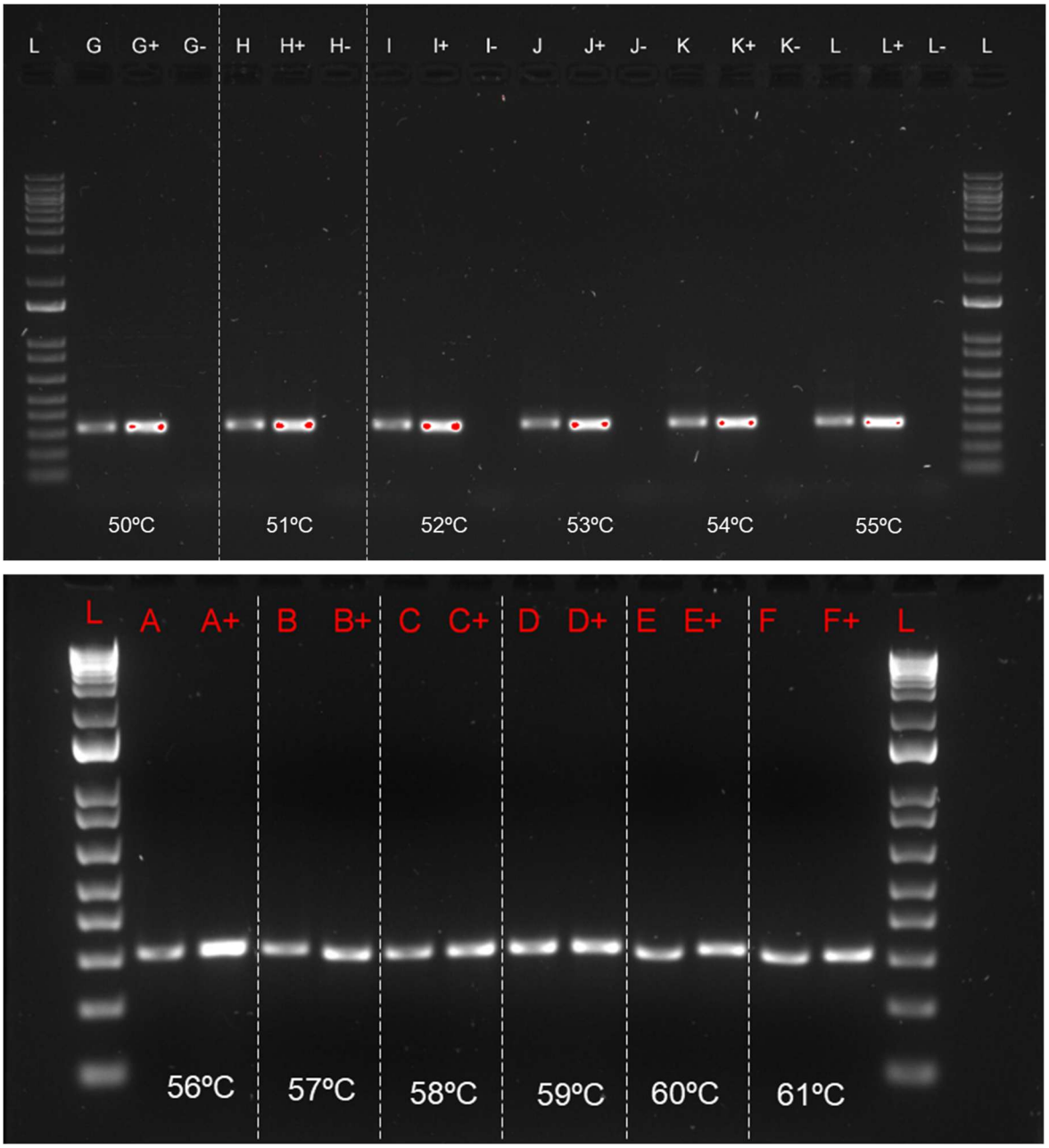

Figure S 5 Gradient PCR of ureC F&R primer (Collins et al., 1999) on environmental soil DNA sample over annealing temperature range 50-61˚C. Column well IDs without, with plus (+) and negative (-) signs indicate environmental DNA sample, environmental DNA sample spiked with 1 µL ureC standard and control PCR water, respectively. "L" stands for ladder used to estimate the base pair (bp) length of the target gene.

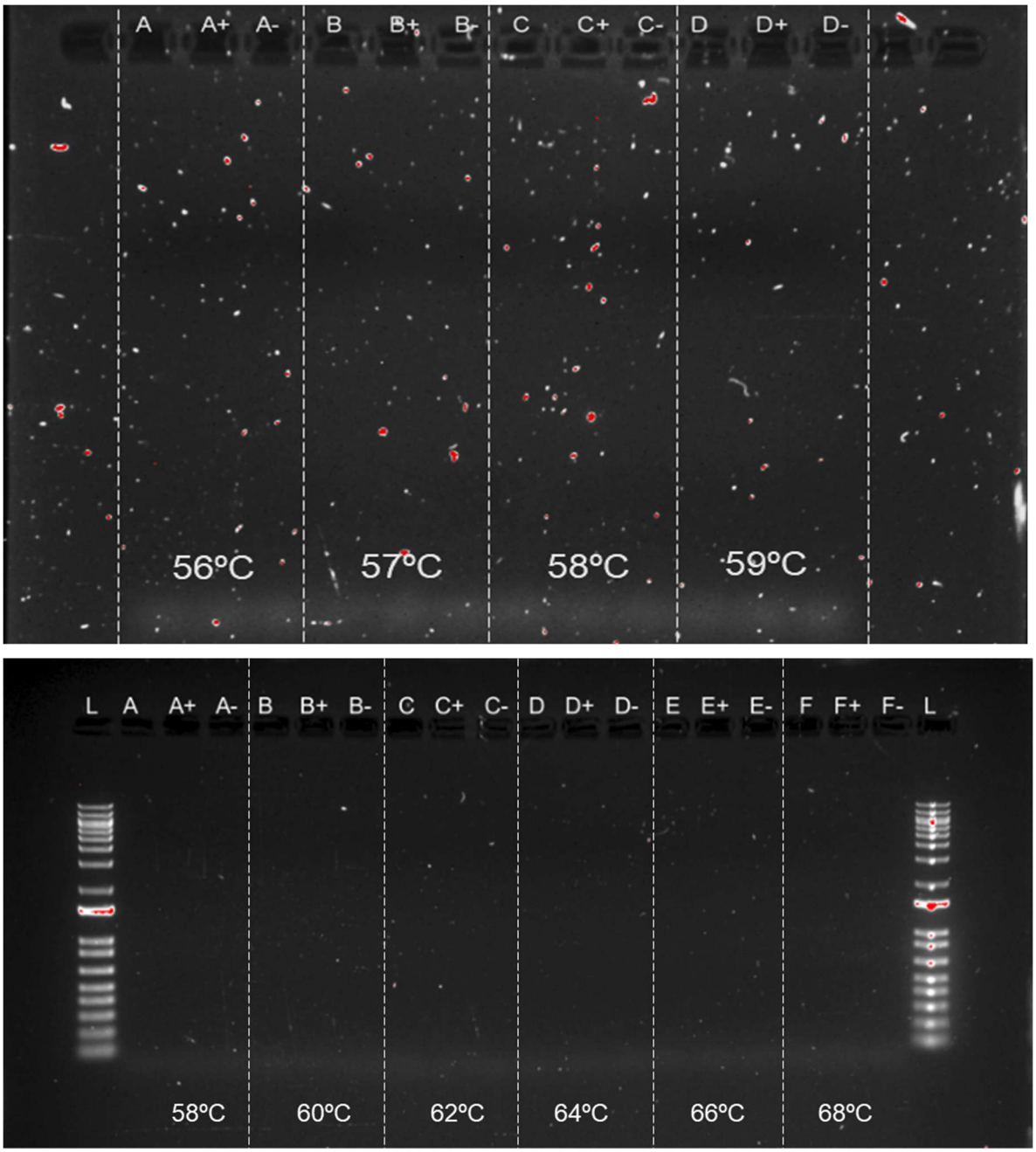

Figure S 6 Gradient PCR of ureC 2LF&R primer (Gresham et al., 2007) on environmental soil DNA sample over annealing temperature range 58-68˚C. Column well IDs without, with plus (+) and negative (-) signs indicate environmental DNA sample, environmental DNA sample spiked with 1 µL ureC standard and control PCR water, respectively. "L" stands for ladder used to estimate the base pair (bp) length of the target gene.

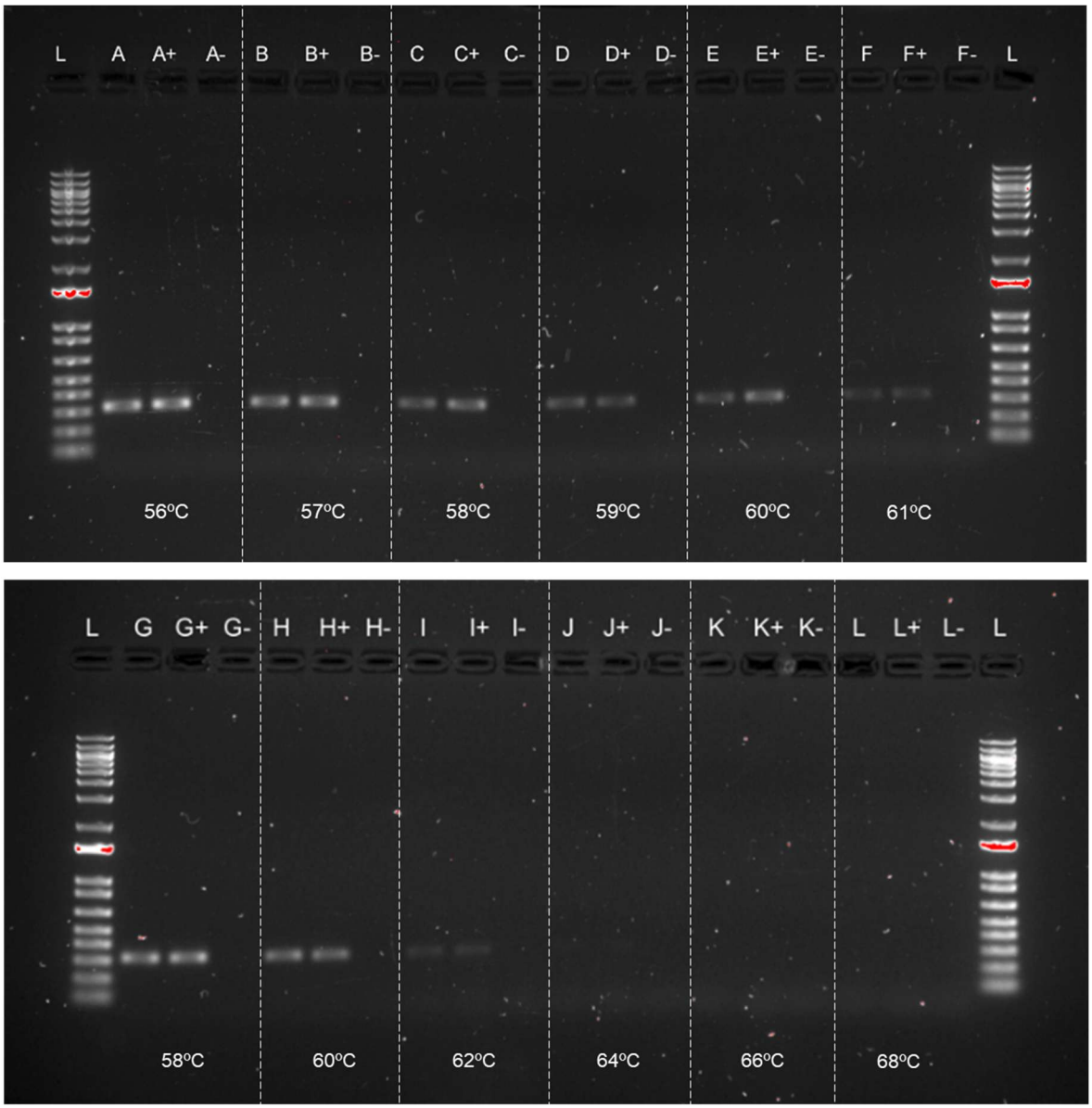

Figure S 7 Gradient PCR of ureC 607F&898R primer (Wang et al., 2022) on environmental soil DNA sample over annealing temperature range 58-68˚C. Column well IDs without, with plus (+) and negative (-) signs indicate environmental DNA sample, environmental DNA sample spiked with 1 µL ureC standard and control PCR water, respectively. "L" stands for ladder used to estimate the base pair (bp) length of the target gene

3. Urease activity assay

3.1. Linear regression model EC v time

Table S 3 Glycine max linear regression model of EC vs time.

ID	Urease	Urea	HC	Dil	r	intercept	slope	std.err	r.sqr	p.value	QCcor	sig	UAmean	UAsd
0 0 0	0	0	0	0	0.39	3.7	0.27	0.14	0.15	7.03E-02	low		5.99	3.13
0 666 0	0	666	0	0	0.48	6.3	0.43	0.40	0.23	3.40E-01	low		9.53	8.81
0 666 10	0	666	10	0.1	0.31	108.1	0.38	0.27	0.10	1.77E-01	low		8.46	6.02
0 666 100	0	666	100	0.01	0.06	15.5	0.04	0.15	0.00	7.92E-01	low		0.90	3.37
0 666 1000	0	666	1000	0.001	0.65	7.2	0.15	0.09	0.42	1.63E-01	low		3.39	1.98
0 666 2.5	0	666	2.5	1	-0.11	773.0	-0.47	2.04	0.01	8.30E-01	low		-10.36	45.18
0 666 5	0	666	5	0.2	0.16	164.5	0.03	0.08	0.02	7.68E-01	low		0.59	1.87
1 0 0	1	0	0	0	0.02	37.5	0.01	0.13	0.00	9.46E-01	low		0.19	2.79
1 666 0	1	666	0	0	0.92	47.3	5.16	0.33	0.85	3.72E-19	high	sign	114.47	7.30
1 666 10	1	666	10	0.1	0.85	145.5	3.71	0.34	0.73	6.17E-14	med	sign	82.44	7.64
1 666 100	1	666	100	0.01	0.86	58.4	4.58	0.42	0.75	8.65E-14	med	sign	101.61	9.25
1 666 1000	1	666	1000	0.001	0.92	50.6	4.71	0.29	0.85	5.57E-20	high	sign	104.58	6.53
1 666 2.5	1	666	2.5	1	0.82	786.9	2.00	0.20	0.68	7.91E-13	med	sign	44.47	4.54
1 666 5	1	666	5	0.2	0.98	203.4	2.32	0.07	0.96	8.98E-33	high	sign	51.49	1.55
100 0 0	100	0	0	0	0.11	2303.1	0.87	1.91	0.01	6.53E-01	low		19.40	42.39
100 666 0	100	666	0	0	0.91	3124.9	203.63	13.71	0.84	1.56E-18	high	sign	4520.56	304.44
100 666 10	100	666	10	0.1	0.90	3122.6	215.73	15.66	0.81	1.45E-17	high	sign	4789.11	347.63
100 666 100	100	666	100	0.01	0.91	3097.8	212.35	14.92	0.82	7.18E-18	high	sign	4714.23	331.29
100 666 1000	100	666	1000	0.001	0.90	3145.4	214.55	15.32	0.82	7.99E-18	high	sign	4762.94	340.03
100 666 2.5	100	666	2.5	1	1.00	3690.0	196.70	1.16	1.00	6.27E-66	high	sign	4366.65	25.82
100 666 5	100	666	5	0.2	1.00	3027.9	203.49	2.92	0.99	1.85E-47	high	sign	4517.48	64.92

Table S 4 Sporosarcina Pasteurii linear regression model of EC vs time.

ID	OD600	Urea	HC	Dil	r	intercept	slope	std.err	r.sqr	p.value	QCcor	sig	UAmean	UAsd
0 666 10	0	666	10	0.1	-0.69	3000	-1.848	0.180	0.478	6.47E-18	low	sign	-41.01	4.00
0 666 100	0	666	100	0.01	0.94	2881	2.205	0.158	0.891	5.05E-13	high	sign	48.96	3.50
0 666 2.5	0	666	2.5	1	0.75	3578	1.884	0.157	0.558	4.30E-22	med	sign	41.82	3.47
0 666 5	0	666	5	0.2	0.57	3044	1.250	0.170	0.320	3.07E-11	low	sign	27.74	3.77
0.01 0 0	0.01	0	0	0	-0.11	2888	-0.202	0.167	0.013	2.28E-01	low		-4.48	3.70
0.01 666 0	0.01	666	0	0	0.29	2438	1.379	0.431	0.086	1.80E-03	low	sign	30.62	9.57
0.01 666 10	0.01	666	10	0.1	0.96	2764	1.587	0.480	0.916	1.87E-01	high		35.22	10.65
0.01 666 100	0.01	666	100	0.01	0.98	2398	1.084	0.025	0.962	1.70E-53	high	sign	24.05	0.56
0.01 666 2.5	0.01	666	2.5	1	0.31	3672	0.623	0.548	0.097	2.78E-01	low		13.83	12.17
0.01 666 5	0.01	666	5	0.2	0.80	2711	2.108	0.342	0.633	3.31E-06	med	sign	46.80	7.59
1 0 0	1	0	0	0	-0.76	3387	-1.763	0.416	0.580	9.72E-04	low	sign	-39.15	9.24
1 666 0	1	666	0	0	0.99	3536	94.685	1.161	0.989	3.23E-74	high	sign	2102.02	25.78
1 666 10	1	666	10	0.1	1.00	2998	86.606	0.370	0.999	5.66E-108	high	sign	1922.65	8.21
1 666 100	1	666	100	0.01	1.00	3292	80.459	0.650	0.993	8.96E-121	high	sign	1786.20	14.43
1 666 2.5	1	666	2.5	1	0.99	3799	65.155	0.625	0.990	2.47E-113	high	sign	1446.45	13.88
1 666 5	1	666	5	0.2	1.00	3173	78.921	0.136	1.000	2.79E-201	high	sign	1752.04	3.01

3.2. Statistical analysis

Table S 5 Glycine max ANOVA and multiple pairwise-comparisons between the means of groups. Results of LSD (Least Significant Difference) test on ANOVA.

ENZYME CONCENTRATION = 1 g/L		
ANOVA p = 4.24e-05 ***		
$groups		
HC	slope	groups
0	5.00039	a
1000	4.86739	a
100	4.58799	a
10	3.58599	b
5	2.29679	c
2.5	2.00294	c
ENZYME CONCENTRATION = 100 g/L		
ANOVA p = 0.881		
$groups		
HC	slope	groups
100	212.9493	a
1000	212.231	a
10	211.9708	a
0	208.4268	a
5	203.3631	a
2.5	196.6961	a

Table S 6 Sporosarcina Pasteurii ANOVA and multiple pairwise-comparisons between the means of groups. Results of LSD (Least Significant Difference) test on ANOVA.

CELL CONCENTRATION = 0.01		
ANOVA p = 0.131		
$groups		
	slope	groups
5	2.197416	a
10	1.586502	ab
0	1.426494	ab
100	1.081262	b
2.5	1.007535	b
CELL CONCENTRATION = 1		
ANOVA p = 5.01e-05 ***		
$groups		
	slope	groups

0	94.68267	a
10	86.52793	b
100	80.52324	bc
5	78.92065	c
2.5	65.19964	d